Electronic Supplementary Material (ESI) for Green Chemistry.

Supporting Information

Composition control of Pd-based bimetallic alloys to boost selective hydrogenation of furfural in aqueous micelles

Yiru Chen[a #], Xi He[a #], Ming Zhang[b], Lixin Chen[a], Xuemin Liu[a], Bing Liu*[a], Hengquan Yang*[b] and Xin Ge*[a]

[a] Key Laboratory of Synthetic and Biological Colloids, Ministry of Education, School of Chemical and Material Engineering, Jiangnan University, Wuxi 214122, P.R China.

[b] School of Chemistry and Chemical Engineering, Shanxi University, Taiyuan 030006, P.R China.

E-mail: liubing@jiangnan.edu.cn; hqyang@sxu.edu.cn; gexin@jiangnan.edu.cn

[#] These authors contributed equally to this work.

Table of contents

Experimental Section

1. Chemicals and Characterization

M2070 (AR) was purchased from Shanghai Huntsman Co., Ltd. D-anhydrous glucose (AR), benzaldehyde (99%), $NaBH_4$ (97%), α-Lactose monohydrate (AR), glucolactone (AR), Tween-60 (AR) were purchased from Sinopharm Chemical Reagent Network. Na_2PdCl_4 (AR), $CuCl_2$ (AR), $NiCl_2$ (AR), SDS (AR), CTAB (AR), polyvinyl pyrrolidone (AR), cinnamaldehyde (99%), 5-methylfurfural (99%), 5-hydroxymethyl furaldehyde (98%), 5-Chlorofurfural (98%), 2-pyridinecarboxaldehyde (98%), vanillin (99%), nitrobenzene (99%) were purchased from Adamas Reagent Network. Ethyl acetate (AR), ethanol (AR), methanol (AR) were purchased from Shanghai Titan Technology Co. Ltd. Furfural (99%), Raney nickel, 2-furylacrolein (98%) were purchased from Energy Chemical Network.

Transmission electron microscopy (TEM, JEM-2100plus) and high-resolution transmission electron microscopy (HRTEM, JEM-2100F) were used to observe the microstructure and lattice fringe length of the catalyst. High Angle Angular Dark Field-Scanning Transmission Electron Microscopy (HAADF-STEM, Titan G2 60-300) was used to analyze the metal elements and metal ratio of the catalyst to prove the successful preparation of the alloy catalyst. X-ray diffractometer (XRD, D2 PHASER) was used to analyze the phase of catalysts with different alloy ratios to further verify the successful preparation of alloy catalysts. The scanning range of 2θ angle was 5 ~ 90 °, and the scanning rate was 10 °/min. X-ray photoelectron spectroscopy (XPS, Axis supra) was used to further characterize the types and valence states of metal elements, and the energy resolution of XPS was 0.48 eV. The ALV/DLS/SLS-5022F laser light scattering system was used to prove the solubilization of the quasi-homogeneous catalytic system for organic substrates and the particle size of the micelles in different concentrations of surfactant aqueous solutions. The reaction mechanism of alloy samples containing furfural at different temperatures was investigated by Thermo IS 50 in-situ infrared spectrometer under hydrogen atmosphere.

All the spin-polarized density functional theory (DFT) calculations were performed by using the Vienna ab-initio simulation package (VASP).[1,2] The van der Waals (vdW) interactions were taken into account when calculating the reaction energetics by using the DFT-D3 approach.[3] The projector-augmented wave (PAW) method was used to represent core-valence interactions.[4] The generalized gradient approximation (GGA) with the Perdew-Burke-Ernzerhof (PBE) functional was used to model electronic exchange and correlation.[5] Valence electrons were described by a plane wave basis with an energy cutoff of 400 eV. Electron smearing was employed via the Methfessel-Paxton technique with a smearing width consistent to 0.2 eV. The convergence criteria for force and energy were set to 0.03 eV/Å and 10-5 eV, respectively. The gamma-centered 1×1×1 k-point mesh was employed for the integration of the Brillouin zone. Transition states (TSs) for the elementary reactions were located using the climbing-image nudged elastic band (CI-NEB) method.[6,7] The optimized transition states were further verified as having a single imaginary frequency.

According to the HRTEM characterization results, the surface hydrogenation reaction of furfural was studied on Pd_1Cu_9(110) surface and Pd_1Ni_3(111) surface. The Pd_1Cu_9(110) surface was modeled using a 3×2 supercell slab with six atomic layers, containing 9 Pd atoms and 81 Cu atoms. The Pd1Ni3(111) surface was modeled using a 6×6 supercell slab with four atomic layers, containing 36 Pd atoms and 108 Ni atoms. The 15 Å vacuum gap perpendicular to the surface was added to separate the neighboring slabs in z-direction.

2. The synthesis of sugar-based surfactants (GluM, LacM, GluLM)

Preparation of GluM：20.0 g polyether amine M2070 and 1.8 g glucose were dissolved in 100 mL anhydrous methanol. The mixed solution was stirred at 50 °C for 24 h to fully react. After the reaction was completed, the mixture was recrystallized 5 times, and the supernatant was taken for vacuum rotary evaporation to obtain a white viscous liquid. The yield of GluM was 85%.

Preparation of LacM：3.80 g α-Lactose monohydrate was dissolved in 60 mL water, and 20.0 g polyether amine M2070 was dissolved in 100 mL isopropanol. The two solutions were mixed and stirred at 80 °C for 24 h to fully react. After the reaction was completed, the mixture was recrystallized 5 times, and the supernatant was taken for vacuum rotary evaporation to obtain a brown viscous liquid. The yield of LacM was 85%.

Preparation of GluLM：1.78 g glucolactone and 20.0 g polyether amine M2070 were dissolved in 100 mL anhydrous methanol. The mixed solution was stirred at 80 °C for 24 h to fully react. After the reaction was completed, the mixture was recrystallized 5 times, and the supernatant was taken for vacuum rotary evaporation to obtain a yellow viscous liquid. The yield of GluLM was 82%.

3. Preparation of bimetallic alloy catalyst

PdCu alloy catalyst: 0.04 mL Na_2PdCl_4 aqueous solution (0.1 mmol/mL) and 0.36 mL $CuCl_2$ aqueous solution (0.1 mmol/mL) were mixed in 9.0 mL GluM aqueous solution (contained 0.2 mmol GluM). Then, the surfactant was vigorously stirred for 5 minutes to fully encapsulate the metal ions. 0.6 mL sodium borohydride aqueous solution (0.1 mmol/mL) was added to the mixed solution under stirring conditions, and the reduction reaction was performed for 10 min. And a uniform and stable black solution was obtained as catalyst for hydrogenation reaction. According to the proportion of metal precursors, the catalyst was used as Pd_1Cu_9.

PdNi alloy catalyst: 0.1 mL Na_2PdCl_4 aqueous solution (0.1 mmol/mL) and 0.30 mL $NiCl_2$ aqueous solution (0.1 mmol/mL) were mixed in 9.0 mL GluM aqueous solution (contained 0.2 mmol GluM). Then, the surfactant was vigorously stirred for 5 minutes to fully encapsulate the metal ions. 0.6 mL sodium borohydride aqueous solution (0.1 mmol/mL) was added to the mixed solution under stirring conditions, and the reduction reaction was performed for 10 min. And a uniform and stable black solution was obtained as catalyst for hydrogenation reaction. According to the proportion of metal precursors, the catalyst was used as Pd_1Ni_3.

4. Selective hydrogenation of furfural

Selective hydrogenation of furfural on Pd_1Cu_9: Take the above black solution 5 mL, diluted it to 20 mL with surfactant aqueous solution. Since the catalyst was uniformly dispersed, the amount of catalyst was determined by the amount of solution taken. 2 mmol cinnamaldehyde was added to the diluted catalyst solution, and then the alloy catalyst solution containing cinnamaldehyde was placed in a high-pressure reactor. Nitrogen and hydrogen were used to replace the gas in the reactor three times, and finally the hydrogen pressure was maintained at 1.0 MPa. After the reaction, the organic matter was extracted with ethyl acetate and dried with anhydrous Na_2SO_4, and the crude product was obtained by vacuum concentration. Crude products were purified by silica gel column chromatography (eluent: ethyl acetate/petroleum ether) to obtain the corresponding pure products, and characterized by ^1H NMR and ^{13}C NMR. The quantification of products were determined based on GC data using external standard method. The conversion of furfural (mol%) and selectivity (mol%) of furfuryl alcohol were calculated as below.

$$FF\ Conversion(\%) = \left(1 - \frac{moles\ of\ furfural}{moles\ of\ furfural\ loaded\ initially}\right) \times 100\%$$

$$FA\ Selectivity\ \ (\%) = \frac{moles\ of\ \ furfuryl\ alcohol}{moles\ of\ furfural\ converted} \times 100\%$$

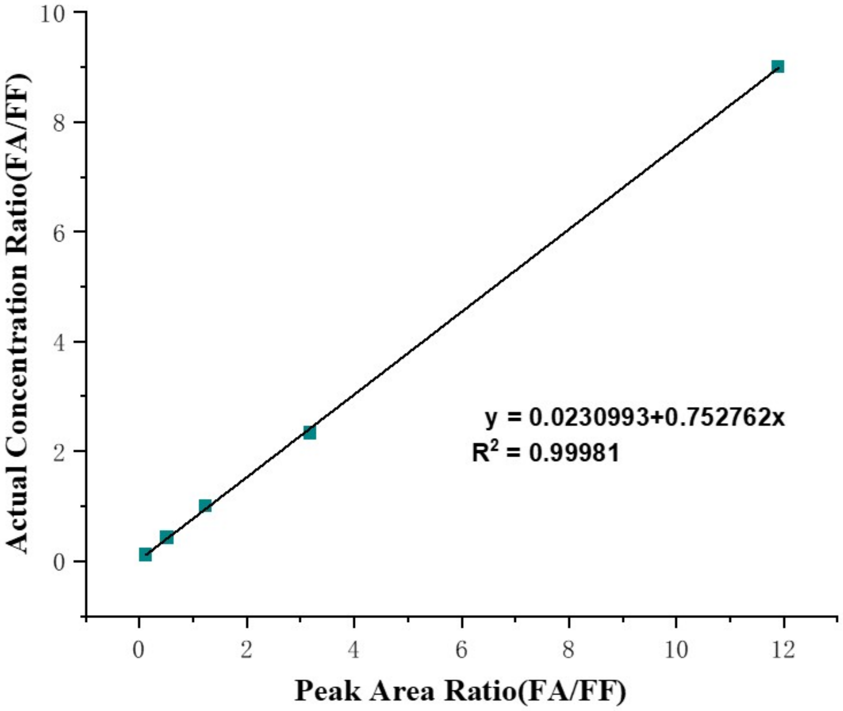

Fig. S1 The standard curve of FA / FF

Hydrogenation of furfural on Pd_1Ni_3: Take the above black solution 10 mL, diluted it to 20 mL with surfactant aqueous solution. Since the catalyst was uniformly dispersed, the amount of catalyst was determined by the amount of solution taken. 2 mmol cinnamaldehyde was added to the diluted catalyst solution, and then the alloy catalyst solution containing cinnamaldehyde was placed in a high-pressure reactor. Nitrogen and hydrogen were used to replace the gas in the reactor three times, and finally the hydrogen pressure was maintained at 1.0 MPa. After the reaction, the organic matter was extracted with ethyl acetate and dried with anhydrous Na_2SO_4, and the crude product was obtained by vacuum concentration. Crude products were purified by silica gel column chromatography (eluent: ethyl acetate/petroleum ether) to obtain the corresponding pure products, and characterized by ^1H NMR and ^{13}C NMR. The quantification of products were determined based on GC data using external standard method. The conversion of furfural (mol%) and selectivity (mol%) of tetrahydrofurfuryl alcohol were calculated as below.

$$FF\ Conversion(\%) = \left(1 - \frac{moles\ of\ furfural}{moles\ of\ furfural\ loaded\ initially}\right) \times 100\%$$

$$THFA\ Selectivity\ (\%) = \frac{moles\ of\ \ tetrahydrofurfuryl\ alcohol}{moles\ of\ furfural\ converted} \times 100\%$$

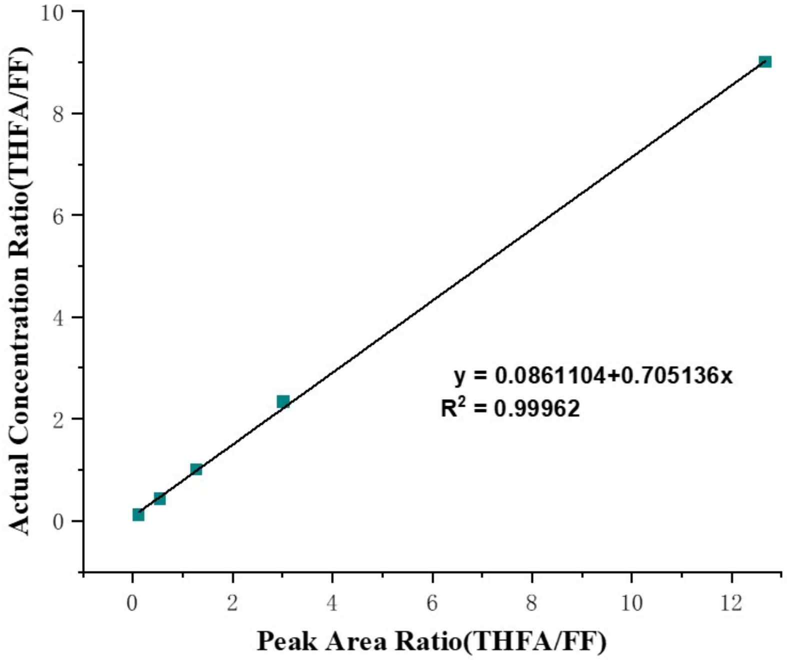

Fig. S2 The standard curve of THFA / FF

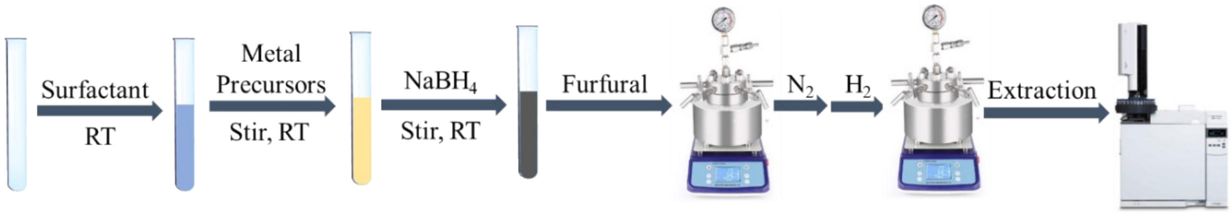

Scheme S1 Preparation of pseudohomogeneous catalyst and catalytic evaluation

5. Optimization of reaction conditions

Table S1 Optimization of conditions for selective hydrogenation of FF.

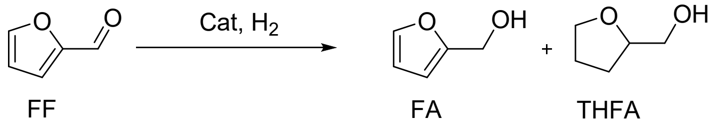

Entry	Catalyst	Surfactant	Conversion/%	Yield $_{FA}$/%	Yield $_{THFA}$/%
1	/	GluM	/	/	/
2	Cu [a]	GluM	14.5	12.9	/
3	Pd [a]	GluM	60.6	56.4	4.2
4	Ni [b]	GluM	44.1	36.9	6.3
5	Pd [b]	GluM	65.6	60.4	5.2

6	Pd_1Cu_9 [a]	PVP	21.2	14.3	6.9
7	Pd_1Cu_9 [c]	GluM	94.4 (99.9) [d]	93.8 (99.8) [d]	0.6 (0.1) [d]

[a] Standard conditions: FF (2.0 mmol), catalyst (0.02 mmol), 5 mM surfactant/H_2O (20 mL) under H_2 (1.0 MPa) at 60 °C for 4 h. [b] catalyst (0.04 mmol), 10 mM surfactant/H_2O (20 mL) at 50 °C. [c] placing the catalytic system in air at room temperature for 24 h. [d] extending the reaction time to 5 h.

Table S2 Screening of surfactant concentration of furfural deep-hydrogenation to THFA [a]

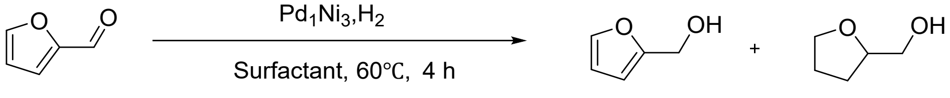

FF FA THFA

Entry	Surfactant Concentration /mM	Conversion/ %	Yield $_{FA}$/%	Yield $_{THFA}$/%	Selectivity $_{FA}$/%
1	5	88.7	25.5	63.2	71.3
2	8	98.1	27.4	70.5	71.9
3	**10**	**99.4**	**3.3**	**95.6**	**96.2**
4	15	99.5	4.8	94.5	95.1
5	20	99.9	7.6	92.1	92.2
6	25	98.9	18.4	80.4	81.3

[a] Reaction conditions: furfural (2.0 mmol), Pd_1Cu_9 (0.02 mmol), surfactant/H_2O (20 mL) under H_2 (1.0 MPa) at 50 °C for 4 h.

Table S3 Screening of reaction temperature of furfural half-hydrogenation to FA [a]

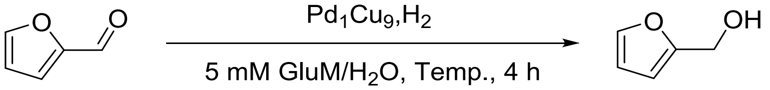

FF FA

Entry	Temperature /°C	Reaction Time/h	Conversion /%	Yield $_{FA}$/%	Yield $_{THFA}$/%	Selectivity $_{FA}$/%
1	100	1	98.5	98.0	0.4	99.5
2	80	3	99.3	98.7	0.3	99.4
3	**60**	**4**	**99.9**	**99.8**	**0.1**	**99.9**
4	50	4	54.9	50.9	4.0	92.7
5	40	4	30.6	24.5	6.1	80.0

[a] Reaction conditions: furfural (2.0 mmol), Pd_1Cu_9 (0.02 mmol), 5 mM surfactant/H_2O (20 mL) under H_2 (1.0 MPa) at 60 °C for 4 h.

Table S4 Screening of hydrogen pressure of furfural half-hydrogenation to FA [a]

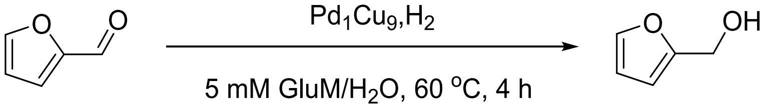

FF FA

Entry	Pressure/	Conversion	Yield $_{FA}$/%	Yield $_{THFA}$/%	Selectivity $_{FA}$/%

	MPa	/%			
1	2.0	99.9	99.0	0.6	99.1
2	1.5	99.9	99.3	0.5	99.4
3	**1.0**	**99.9**	**99.8**	**0.1**	**99.9**
4	0.75	86.3	85.0	1.4	98.4
5	0.50	73.4	71.0	2.4	96.8
6	0.10	22.1	15.3	6.8	69.3

[a] Reaction conditions: furfural (2.0 mmol), Pd_1Cu_9 (0.02 mmol), 5 mM surfactant/H_2O (20 mL) under H_2 at 60 °C for 4 h.

Table S5 Screening of reaction temperature of furfural deep-hydrogenation to THFA [a]

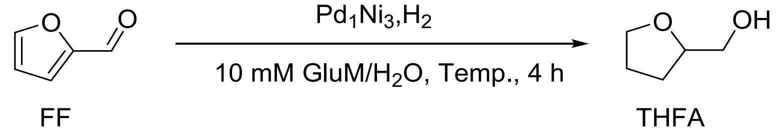

Entry	Temperature /°C	Conversion /%	Yield $_{FA}$/%	Yield $_{THFA}$/%	Selectivity $_{THFA}$/%
1	70	99.4	3.2	93.6	94.2
2	60	99.4	3.3	95.6	96.2
3	**50**	**99.4**	**3.3**	**95.6**	**96.2**
4	40	99.3	21.4	72.3	72.8
5	30	98.2	59.5	38.7	39.4

[a] Reaction conditions: furfural (2.0 mmol), catalyst (0.04 mmol), 10 mM surfactant/H_2O (20 mL) under H_2 (1.0 MPa) for 4 h.

Table S6 Screening of hydrogen pressure of furfural deep-hydrogenation to THFA [a]

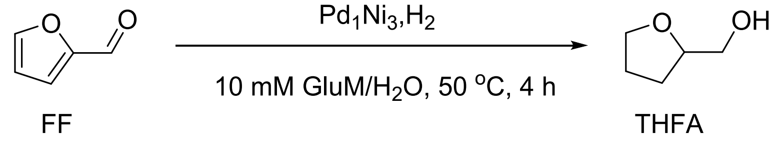

Entry	Pressure/ MPa	Conversion/ %	Yield $_{FA}$/%	Yield $_{THFA}$/%	Selectivity $_{THFA}$/%
1	1.50	99.4	1.3	92.7	93.3
2	1.25	99.4	1.6	92.9	93.5
3	**1.0**	**99.4**	**3.3**	**95.6**	**96.2**
4	0.75	93.9	49.8	38.2	40.7
5	0.50	30.6	20.9	8.4	27.4

[a] Reaction conditions: furfural (2.0 mmol), Pd_1Ni_3 (0.04 mmol), 10 mM surfactant/H_2O (20 mL) under H_2 at 50 °C for 4 h.

Table S7 Reaction process under standard reaction conditions [a]

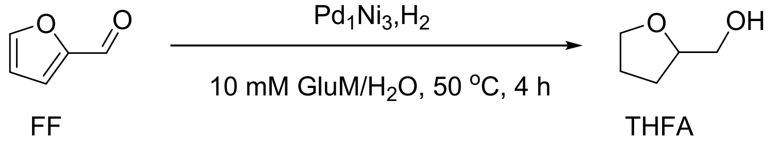

Reaction time/h	Conversion/%	Yield $_{FA}$/%	Yield $_{THFA}$/%
0.5	99.5	73.4	26.0
1.0	99.5	54.3	45.1
1.5	99.4	38.0	61.5
2.0	99.4	28.3	71.2
2.5	99.4	21.3	78.1
3.0	99.4	14.9	84.5
3.5	99.4	8.7	90.7
4.0	**99.4**	**3.3**	**95.6**

[a] Reaction conditions: furfural (2.0 mmol), Pd_1Ni_3 (0.04 mmol), 10 mM surfactant/H_2O (20 mL) under H_2 (1.0 Mpa) at 50 °C.

Table S8 Reaction process at 30 °C [a]

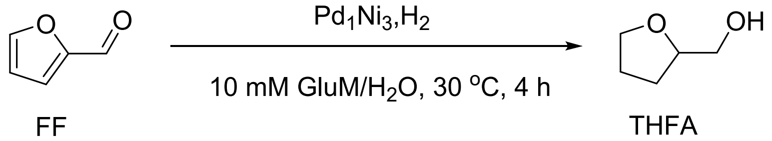

Reaction time/h	Conversion/%	Yield $_{FA}$/%	Yield $_{THFA}$/%
0.5	48.6	41.5	7.0
1.0	94.3	88.7	5.6
1.5	94.6	81.6	12.4
2.0	94.9	77.4	17.5
2.5	97.1	73.7	23.4
3.0	97.6	68.1	29.5
3.5	98.2	64.5	33.7
4.0	98.2	59.5	38.7

[a] Reaction conditions: furfural (2.0 mmol), Pd_1Ni_3 (0.04 mmol), 10 mM surfactant/H_2O (20 mL) under H_2 (1.0 Mpa) at 30 °C.

Table S9 Kinetic experiments of furfural half-hydrogenation to FA [a]

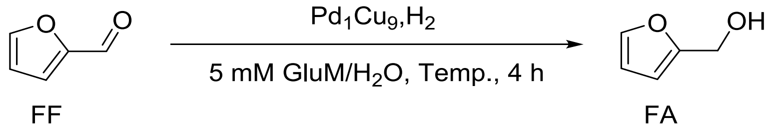

Reaction time/h	40 °C	50 °C	60 °C	70 °C
0	0	0	0	0
0.5	3.2	6.8	13.4	23.4
1.0	8.7	14.7	28.7	45.8
1.5	12.5	23.4	46.7	67.5
2.0	17.1	29.9	60.9	84.5
3.0	21.2	43.4	85.1	99.7
4.0	24.5	50.9	99.8	99.7

5.0	27.7	55.6	99.8	99.7

[a] Reaction conditions: furfural (2.0 mmol), Pd_1Cu_9 (0.02 mmol), 5 mM surfactant/H_2O (20 mL) under H_2 (1.0 MPa) for 4 h.

Table S10 Kinetic experiments of furfural deep-hydrogenation to THFA [a]

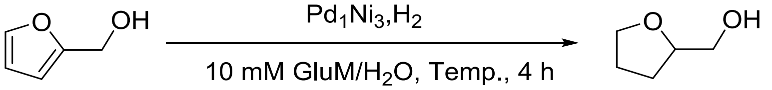

FA THFA

Reaction time/h	30 °C	40 °C	50 °C	60 °C
0	0	0	0	0
0.5	10.4	14.7	30.4	40.5
1.0	21.7	32.1	50.4	60.7
1.5	30.1	47.6	67.9	78.4
2.0	37.7	60.7	80.4	87.4
3.0	43.1	72.1	91.4	93.4
4.0	49.7	80.7	95.4	95.8
5.0	55.4	84.1	95.8	95.8

[a] Reaction conditions: furfuryl alcohol (2.0 mmol), catalyst (0.04 mmol), 10 mM surfactant/H_2O (20 mL) under H_2 (1.0 MPa) for 4 h.

Table S11 Experiments on hydride shuttling [a]

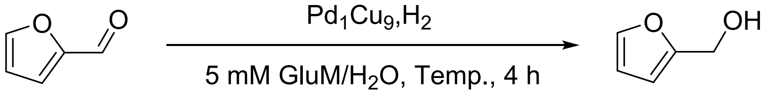

FF FA

Reaction time/h	H_2O/H_2	H_2O/D_2	D_2O/H_2
0	0	0	0
0.5	13.4	11.4	9.2
1.0	28.7	22.4	17.4
1.5	46.7	34.4	27.8
2.0	60.9	50.3	41.3
3.0	85.1	71.7	62.6
4.0	99.8	85.4	77.7
5.0	99.8	95.8	89.8

[a] Reaction conditions: furfural (2.0 mmol), Pd_1Cu_9 (0.02 mmol), 5 mM surfactant/H_2O/D_2O (20 mL) under H_2/D_2 (1.0 MPa) for 4 h.

6. Compound data for alcohols

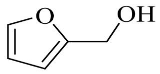

Furfuryl alcohol 2a (0.194 g, 99% isolated yield). ^{1}H NMR (400 MHz, Chloroform-*d*) δ 7.31 (dd, *J* = 1.9, 0.9 Hz, 1H), 6.26 (dd, *J* = 3.2, 1.9 Hz, 1H), 6.20 (d, *J* = 3.3 Hz, 1H), 4.51 (s, 2H), 1.90 (s, 1H). **^{13}C NMR (100 MHz, Chloroform-*d*)** δ 154.15 , 142.68 , 110.48 , 107.85 , 57.57 , 1.14 .

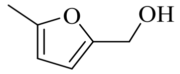

5-Methyl-2-furanmethanol 2b (0.220 g, 99% isolated yield). ^{1}H NMR (400 MHz, Chloroform-*d*) δ 6.16 (d, *J* = 3.1 Hz, 1H), 5.91 (dd, *J* = 3.0, 1.2 Hz, 1H), 4.53 (s, 2H), 2.28 (d, *J* = 0.9 Hz, 3H), 1.88 (s, 1H). **^{13}C NMR (100 MHz, Chloroform-*d*)** δ 151.38 , 151.24 , 107.72 , 105.21 , 56.50 , 12.51 .

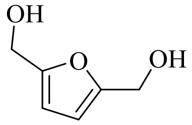

2,5-Furandimethanol 2c (0.253 g, 99% isolated yield). ^{1}H NMR (400 MHz, Chloroform-*d*) δ 6.24 – 6.13 (m, 2H), 4.62 – 4.50 (m, 6H). **^{13}C NMR (100 MHz, Chloroform-*d*)** δ 153.05, 107.55, 56.54.

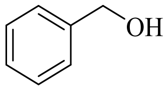

Benzyl alcohol 2d (0.203 g, 94% isolated yield). ^{1}H NMR (400 MHz, Chloroform-*d*) δ 7.36 – 7.16 (m, 5H), 4.59 (s, 2H), 1.81 (s, 1H). **^{13}C NMR (100 MHz, Chloroform-*d*)** δ 139.85 , 127.52 , 126.61 , 125.95 , 64.30 .

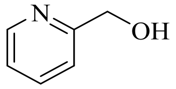

2-Pyridinemethanol 2e (0.202 g, 93% isolated yield). ^{1}H NMR (400 MHz, Chloroform-*d*) δ 8.47 (dt, *J* = 4.9, 1.3 Hz, 1H), 7.61 (td, *J* = 7.7, 1.8 Hz, 1H), 7.24 – 7.17 (m, 1H), 7.17 – 7.08 (m, 1H), 4.69 (s, 2H), 3.75 (s, 1H). **^{13}C NMR (100 MHz, Chloroform-*d*)** δ 158.22 , 147.47 , 135.73 , 121.31 , 119.59 , 63.19 .

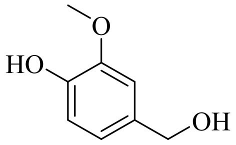

Vanillyl alcohol 2f (0.270 g, 88% isolated yield). ^{1}H NMR (400 MHz, Chloroform-*d*) δ 6.90 – 6.72 (m, 3H), 5.55 (d, *J* = 10.4 Hz, 1H), 4.56 – 4.43 (m, 2H), 3.88 –3.79 (m, 3H). **^{13}C NMR (100 MHz, Chloroform-*d*)** δ 145.65 , 144.27 , 131.94 , 119.22 , 113.25 , 108.94 , 64.46 , 54.91 , 28.68

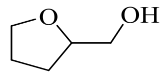

Tetrahydrofurfuryl alcohol 3a (0.194 g, 95% isolated yield). ^{1}H NMR (400 MHz, Chloroform-*d*) δ 3.99 (qd, *J* = 6.8, 3.2 Hz, 1H), 3.90 – 3.80 (m, 1H), 3.76 (dt, *J* = 8.5, 6.8 Hz, 1H), 3.64 (dd, *J* = 11.5, 3.3 Hz, 1H), 3.48 (dd, *J* = 11.6, 6.2 Hz, 1H), 2.31 (s, 1H), 1.98 – 1.81 (m, 3H), 1.71 – 1.54 (m, 1H). **^{13}C NMR (100 MHz, Chloroform-*d*)** δ 78.47 , 67.25 , 63.92 , 26.15 , 25.03 .

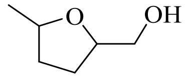

Tetrahydro-5-methyl-2-furanmethanol 3b (0.207 g, 89% isolated yield). ^{1}H NMR (400 MHz, Chloroform-*d*) δ 4.47 (s, 1H), 4.05 (q, *J* = 7.2 Hz, 2H), 2.21 (s, 1H), 1.97 (s, 3H), 1.35 (s, 1H), 1.18 (t, *J* = 7.1 Hz, 4H). **^{13}C NMR (100 MHz, Chloroform-*d*)** δ 59.38 , 56.50 , 29.31 , 19.99 , 13.17 , 12.51

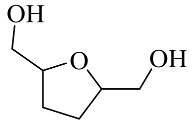

2,5-Bis[hydroxymethyl]tetrahydrofuran 3c (0.238 g, 90% isolated yield). ^{1}H NMR (400 MHz, Chloroform-*d*) δ 4.09 (ddq, *J* = 8.1, 5.4, 3.1, 2.6 Hz, 2H), 3.76 (dd, *J* = 11.8, 2.8 Hz, 2H), 3.56 – 3.40 (m, 2H), 2.00 – 1.86 (m, 2H), 1.86 – 1.71 (m, 2H), 1.24 (s, 1H), 0.85 – 0.77 (m, 1H). **^{13}C NMR (100 MHz, Chloroform-*d*)** δ 79.33 , 63.91 , 26.18 .

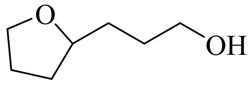

Tetrahydro-2-furanpropanol 3d (0.195 g, 75% isolated yield). ^{1}**H NMR (400 MHz, Chloroform-*d*)** δ 3.89 – 3.72 (m, 2H), 3.68 (t, *J* = 7.8 Hz, 1H), 3.64 – 3.52 (m, 2H), 2.71 – 2.54 (m, 1H), 2.01 – 1.96 (m, 1H), 1.90 – 1.73 (m, 2H), 1.61 (qd, *J* = 5.7, 3.7, 2.8 Hz, 3H), 1.40 (dq, *J* = 11.3, 8.3 Hz, 1H), 1.23 – 1.18 (m, 1H). ^{13}**C NMR (100MHz, Chloroform-*d*)** δ 78.41 , 66.76 , 61.83 , 31.61 , 30.52 , 28.90 , 24.68 .

7. Mechanistic investigation

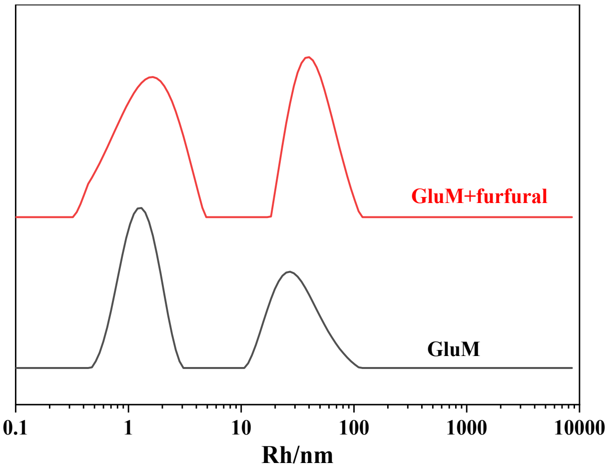

Fig. S3 Particle size distribution of 5 mM GluM aqueous solution before and after adding furfural

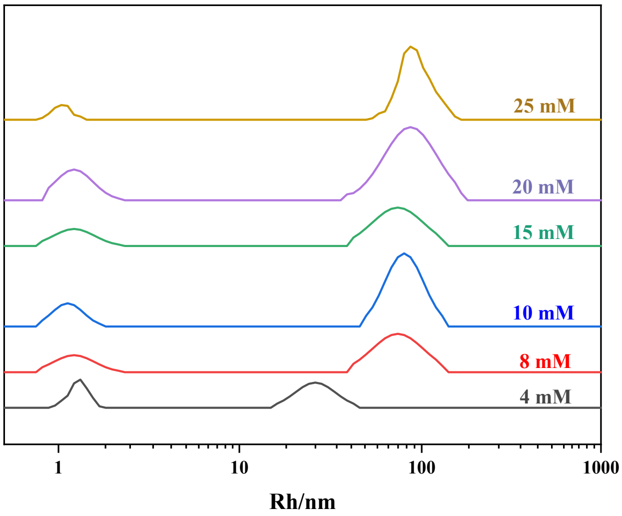

Fig. S4 Particle size distribution of aqueous solutions with different concentrations of GluM

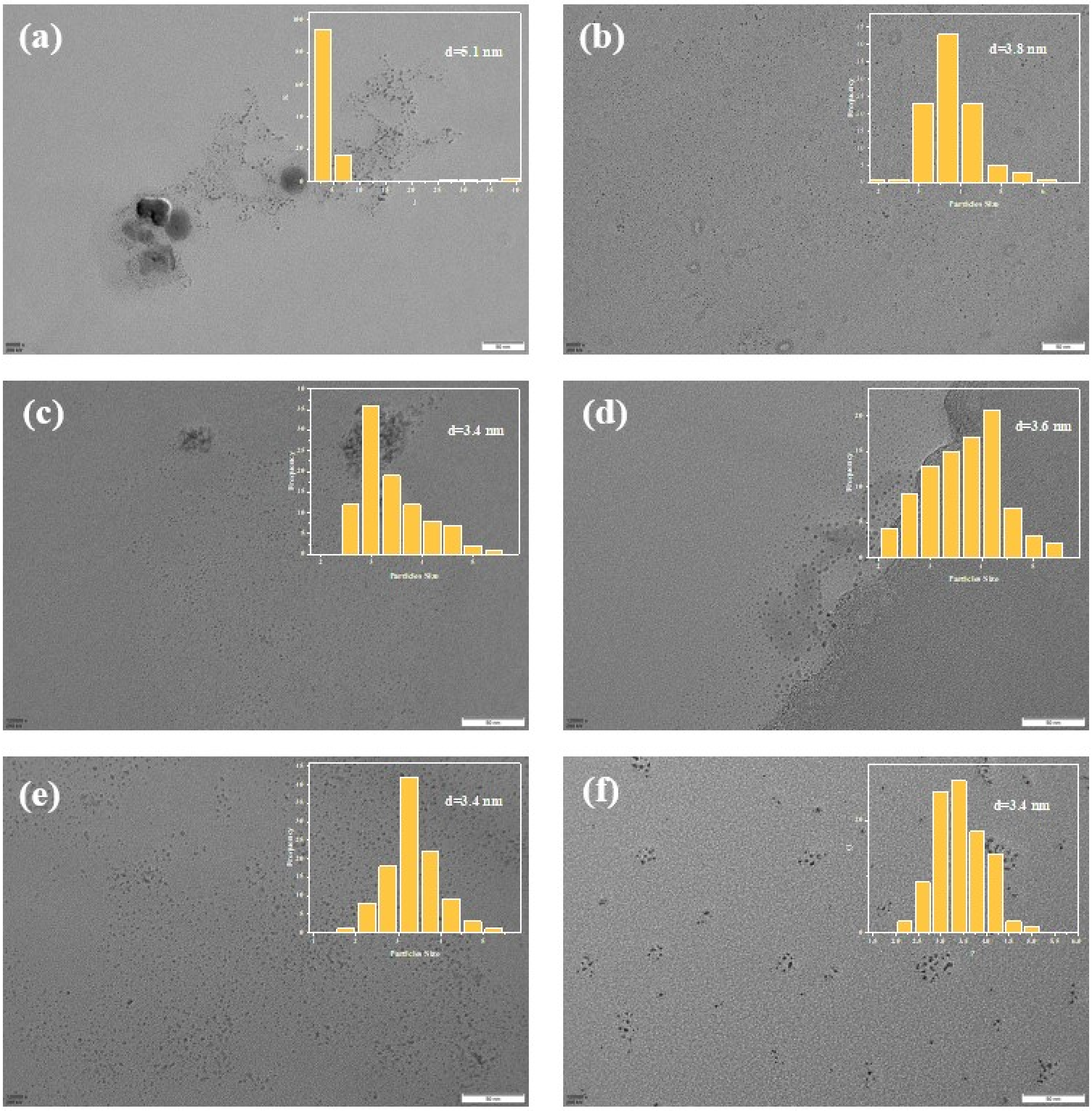

Fig. S5 TEM image of Pd_1Cu_9 alloy catalyst stabilized by SDS (a), CTAB (b), Tween 60 (c), M2070 (d), LacM (e) and GlulM (f)

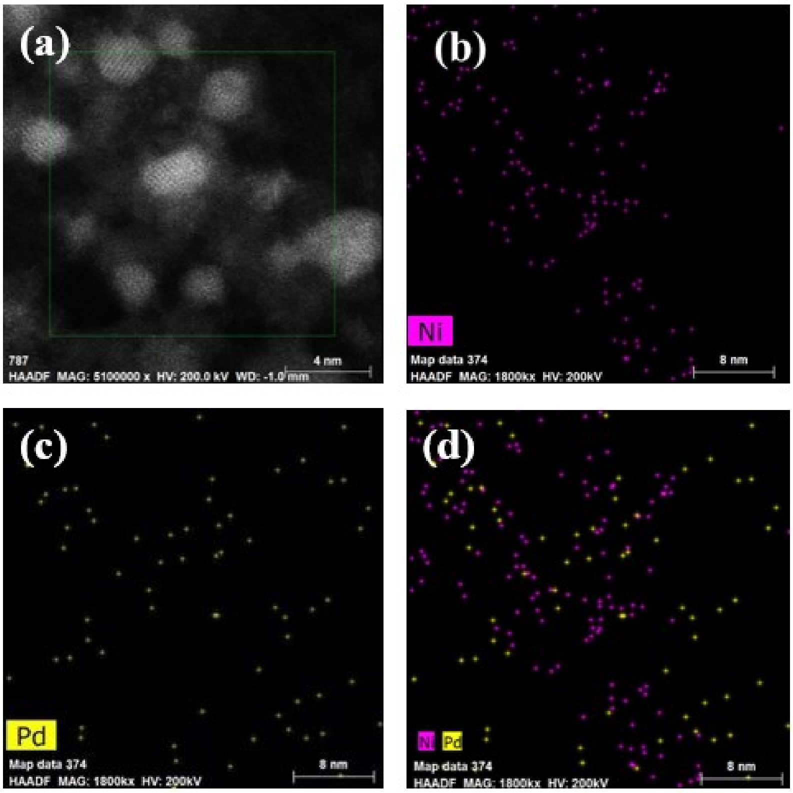

Fig. S6 HAADF-STEM image of Mapping (a, b, c, d) of Pd_1Ni_3 alloy catalyst stabilized by GluM

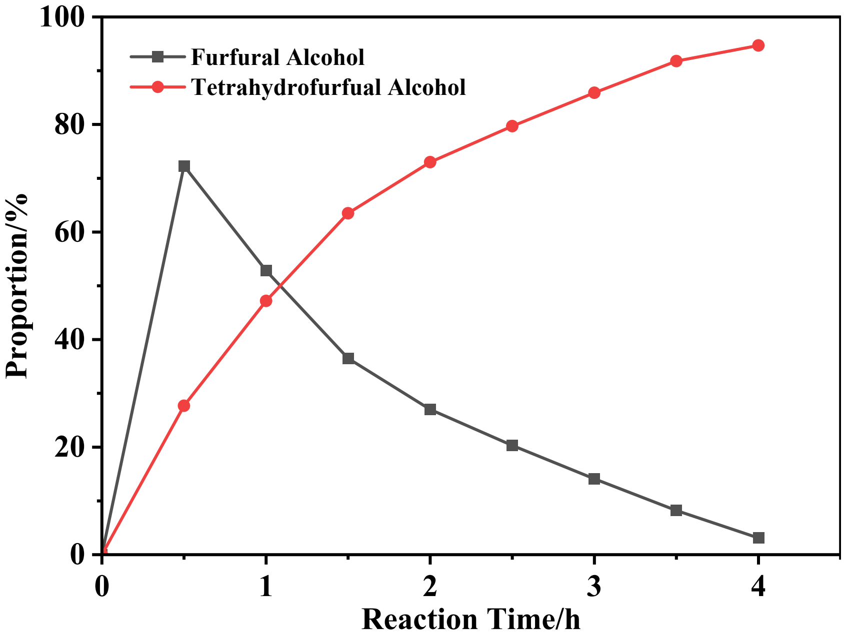

Fig. S7 Reaction process under standard reaction conditions ^{a}

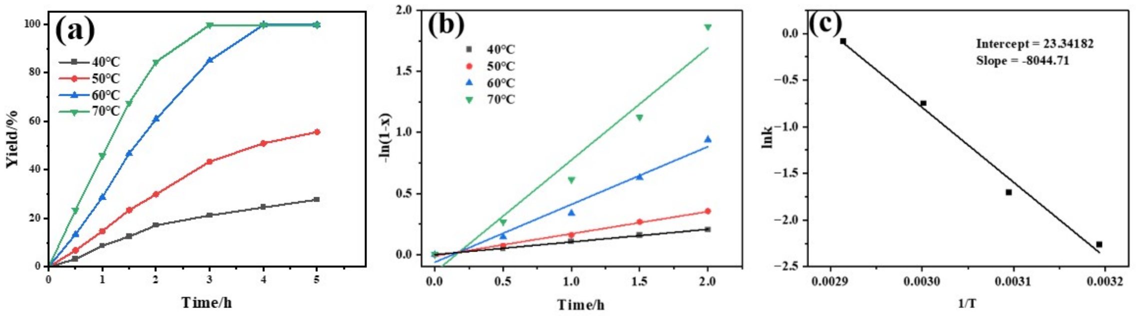

Fig. S8 (a) Reaction rate curve at 40 °C, 50 °C, 60 °C and 70 °C; (b) relationship between FF conversion and reaction time at 40 °C, 50 °C, 60 °C and 70 °C; (c) Relationship between hydrogenation rate k and reaction temperature T at 40 °C, 50 °C, 60 °C and 70 °C

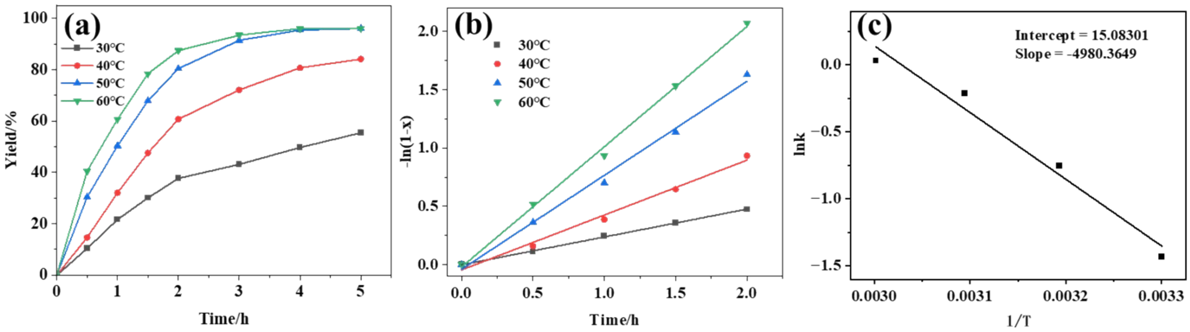

Fig. S9 (a) Reaction rate curve at 30 °C, 40 °C, 50 °C and 60 °C; (b) relationship between FA conversion and reaction time at 30 °C, 40 °C, 50 °C and 60 °C; (c) Relationship between hydrogenation rate k and reaction temperature T at 30 °C, 40 °C, 50 °C and 60 °C

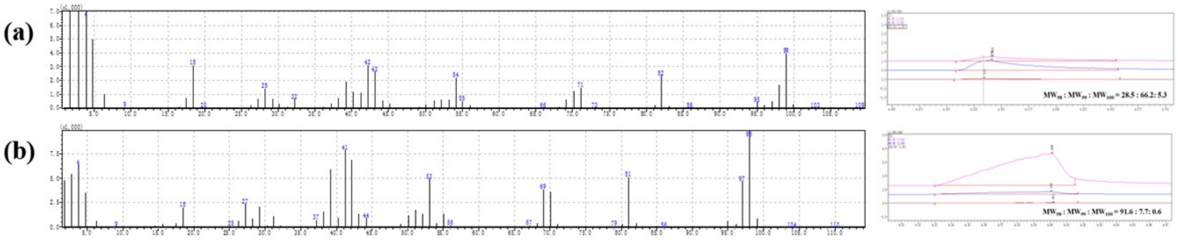

Fig. S10 Mass spectrometry of furfural half-hydrogenation products: (a) replacing H_2 with D_2 and (b) replacing H_2O with D_2O.

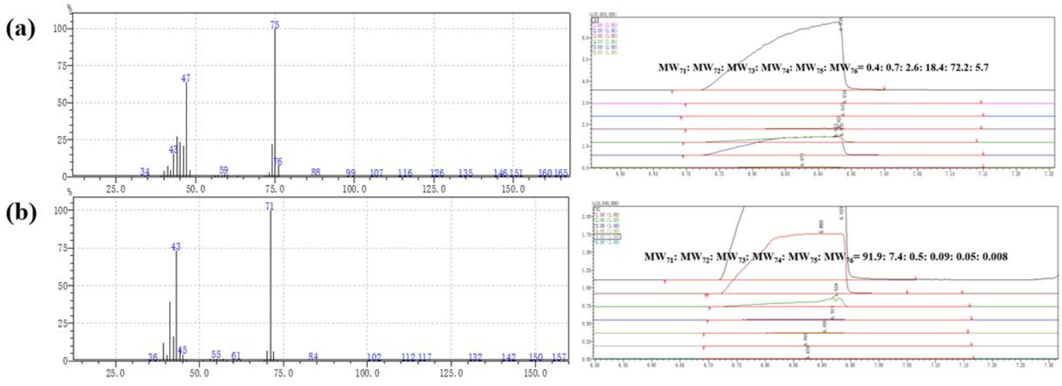

Fig. S11 Mass spectrometry of furfural deep-hydrogenation products: (a) replacing H_2 with D_2 and (b) replacing H_2O with D_2O.

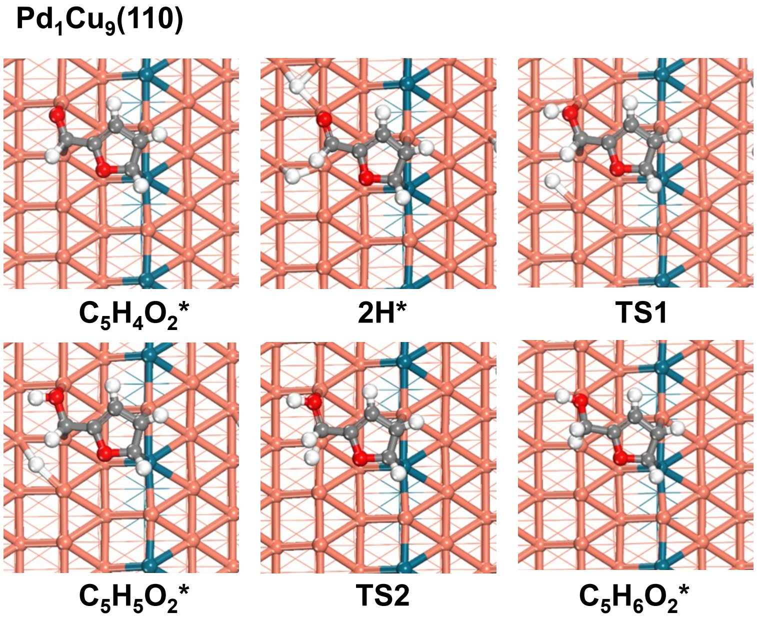

Fig. S12 Calculated structures in the reaction process of Furfural hydrogenation to form furfuryl alcohol on $Pd_1Cu_9(110)$.

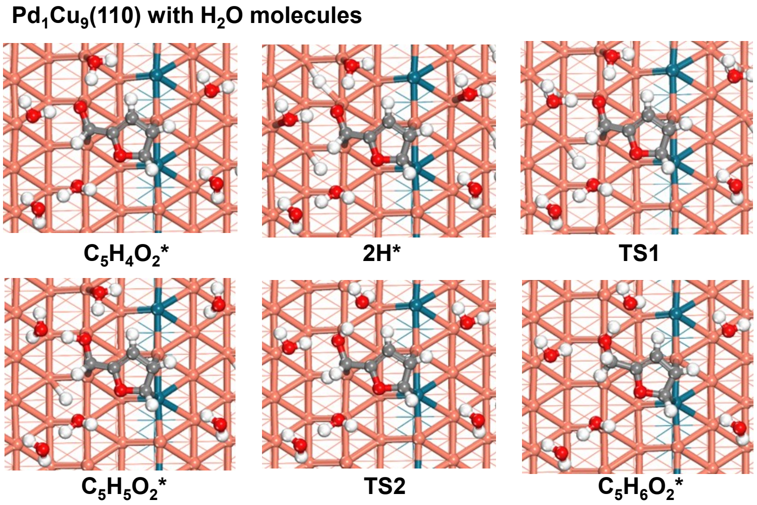

Fig. S13 Calculated structures in the reaction process of furfural hydrogenation to form furfuryl alcohol on H_2O-adsorbed $Pd_1Cu_9(110)$.

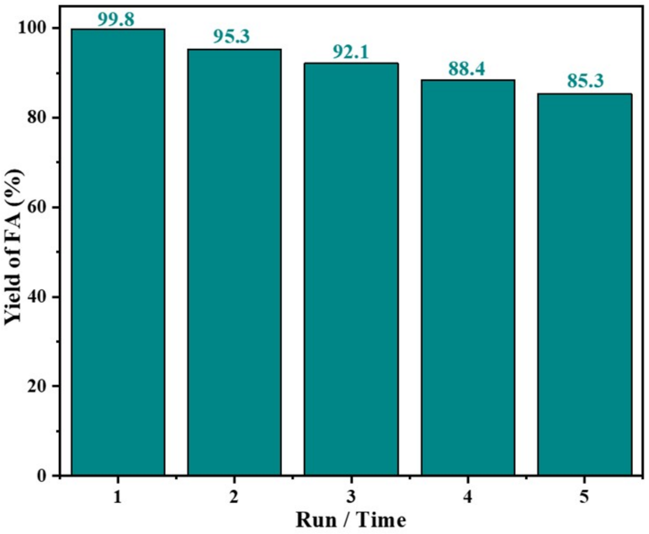

Fig. S14 Recycling and reuse of Pd_1Cu_9 alloy catalysts.

8. Spectra of products

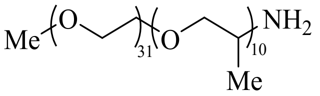

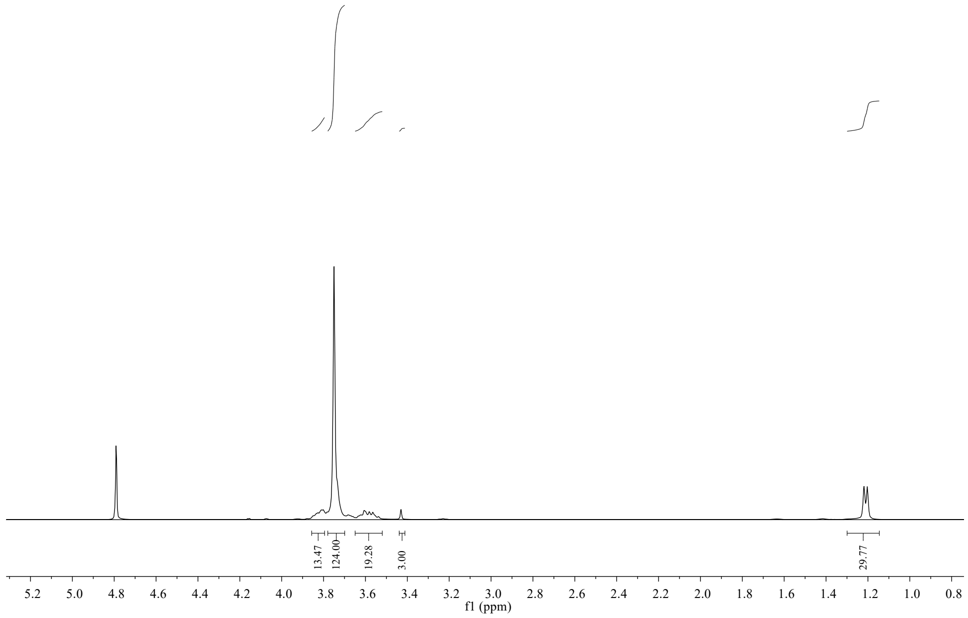

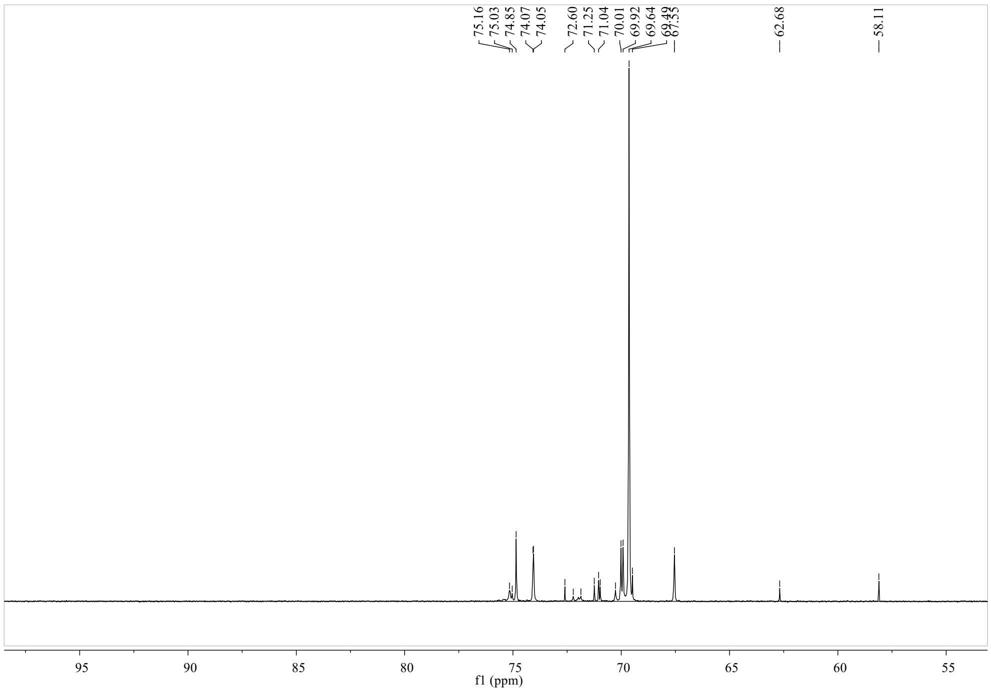

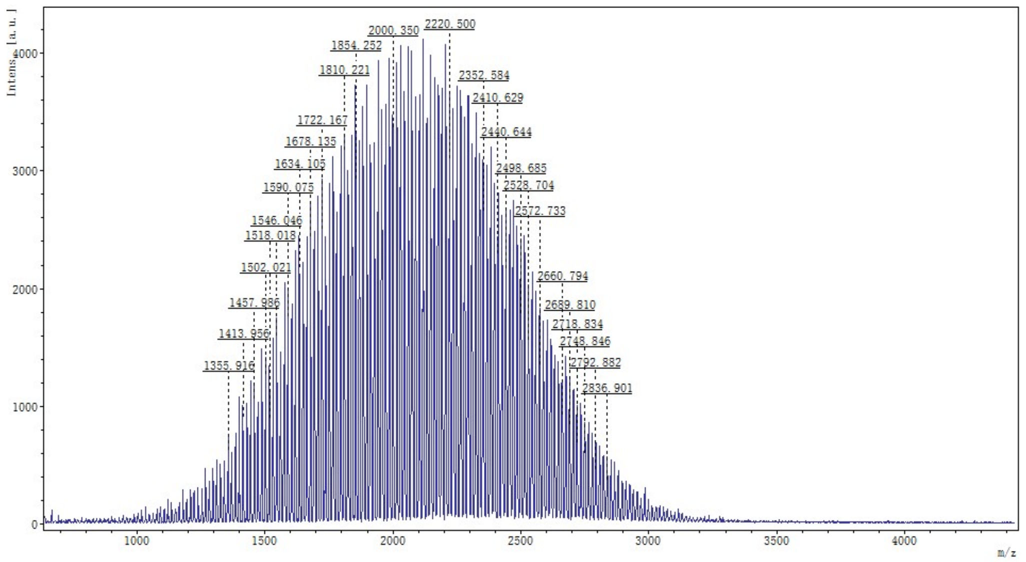
Intens. [a. u.]
4000
3000
2000
1000
0
2000.350
2220.500
1854.252
1810.221
2352.584
2410.629
1722.167
2440.644
1678.135
1634.105
2498.685
1590.075
2528.704
1546.046
2572.733
1518.018
1502.021
2660.794
1457.986
2689.810
1413.956
2718.834
2748.846
1355.916
2792.882
2836.901
1000
1500
2000
2500
3000
3500
4000
m/z

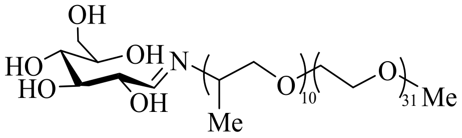
OH
HO
HO
OH
OH
N
O
10
O
31
Me
Me

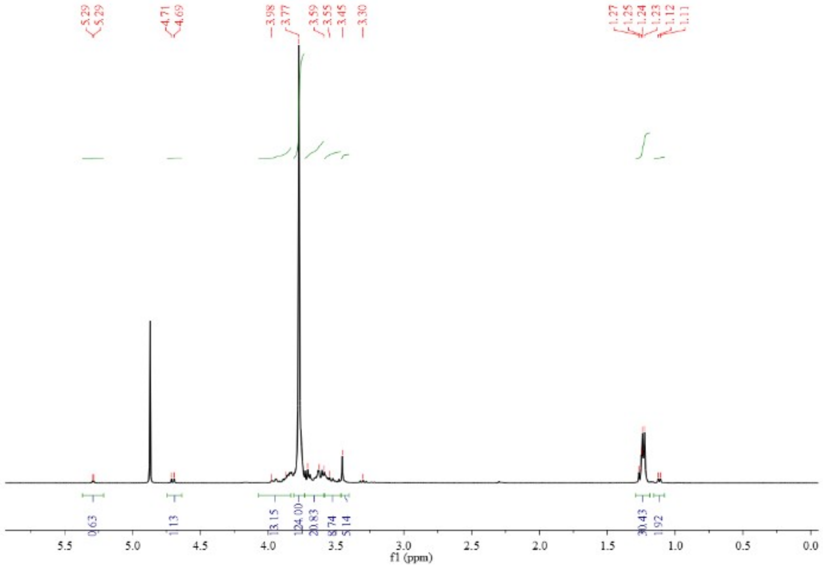
5.29
5.29
4.71
4.69
3.98
3.77
3.59
3.55
3.45
3.30
1.27
1.25
1.24
1.23
1.12
1.11
0.63
1.13
3.15
124.00
20.83
8.74
5.14
30.43
1.92
5.5
5.0
4.5
4.0
3.5
3.0
2.5
2.0
1.5
1.0
0.5
0.0
f1 (ppm)

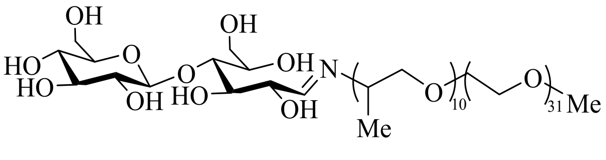
OH
O
HO
HO
OH
O
OH
OH
HO
OH
N
O
10
O
31
Me
Me

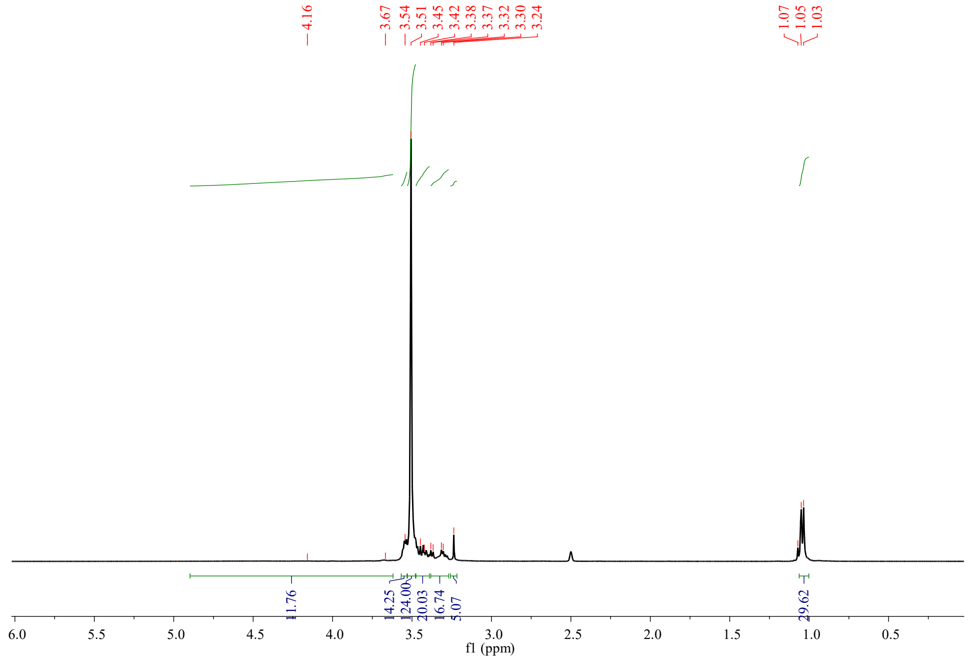
4.16
3.67
3.54
3.51
3.45
3.42
3.38
3.37
3.32
3.30
3.24
1.07
1.05
1.03
11.76
14.25
124.00
20.03
16.74
5.07
29.62
6.0
5.5
5.0
4.5
4.0
3.5
3.0
2.5
2.0
1.5
1.0
0.5
f1 (ppm)

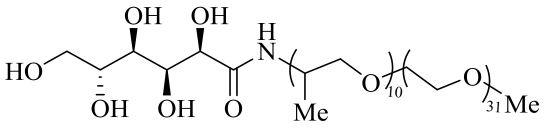
HO
OH
OH
OH
OH
O
H
N
Me
O
10
O
31
Me

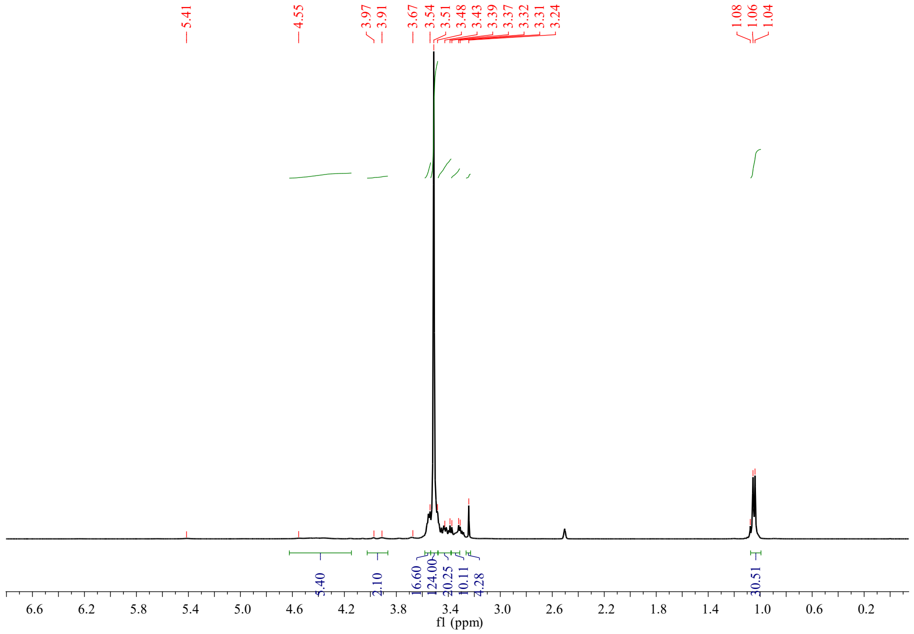
5.41
4.55
3.97
3.91
3.67
3.54
3.51
3.48
3.43
3.39
3.37
3.32
3.31
3.24
1.08
1.06
1.04
5.40
2.10
16.60
124.00
20.25
10.11
4.28
30.51
6.6
6.2
5.8
5.4
5.0
4.6
4.2
3.8
3.4
3.0
2.6
2.2
1.8
1.4
1.0
0.6
0.2
f1 (ppm)

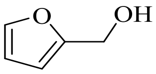
O
OH

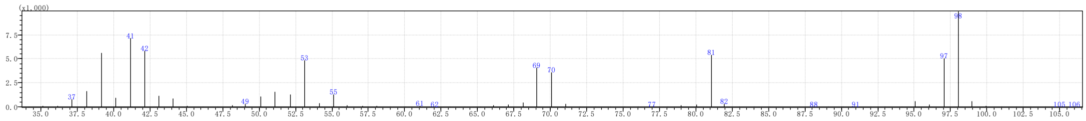
(x1,000)
7.5
5.0
2.5
0.0
37
41
42
49
53
55
61
62
69
70
77
81
82
88
91
97
98
105
106
35.0
37.5
40.0
42.5
45.0
47.5
50.0
52.5
55.0
57.5
60.0
62.5
65.0
67.5
70.0
72.5
75.0
77.5
80.0
82.5
85.0
87.5
90.0
92.5
95.0
97.5
100.0
102.5
105.0

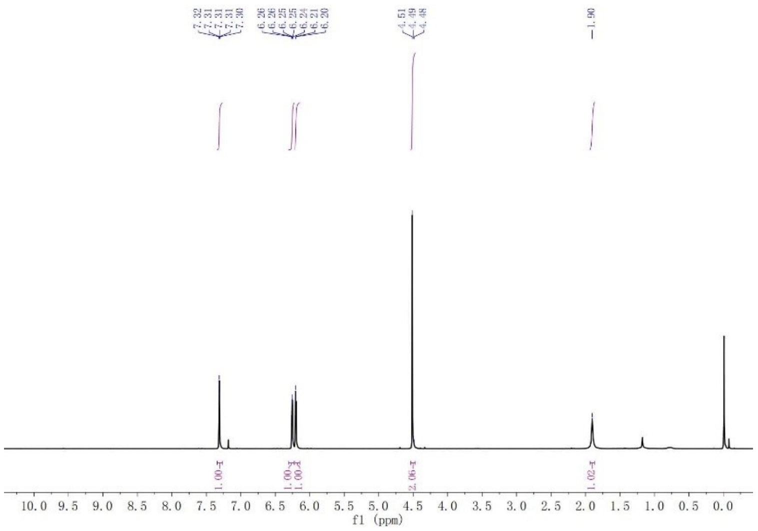
7.32
7.31
7.31
7.31
7.30
6.26
6.26
6.25
6.25
6.24
6.21
6.20
4.51
4.49
4.48
1.90
1.00
1.00
1.00
2.06
1.02
10.0 9.5 9.0 8.5 8.0 7.5 7.0 6.5 6.0 5.5 5.0 4.5 4.0 3.5 3.0 2.5 2.0 1.5 1.0 0.5 0.0
f1 (ppm)

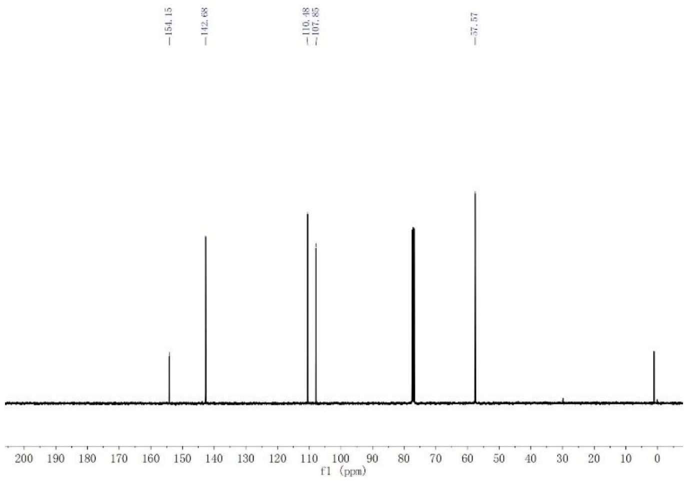
154.15
142.68
110.48
107.85
57.57
200 190 180 170 160 150 140 130 120 110 100 90 80 70 60 50 40 30 20 10 0
f1 (ppm)

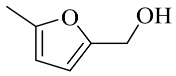
O
OH

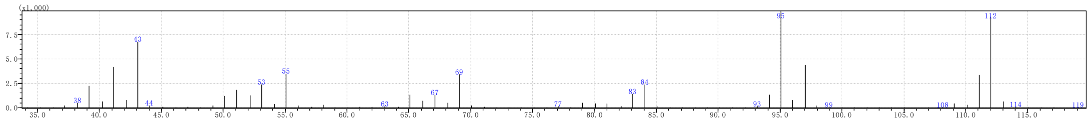
(x1,000)
7.5
5.0
2.5
0.0
38
43
44
53
55
63
67
69
77
83
84
93
95
99
108
112
114
119
35.0 40.0 45.0 50.0 55.0 60.0 65.0 70.0 75.0 80.0 85.0 90.0 95.0 100.0 105.0 110.0 115.0

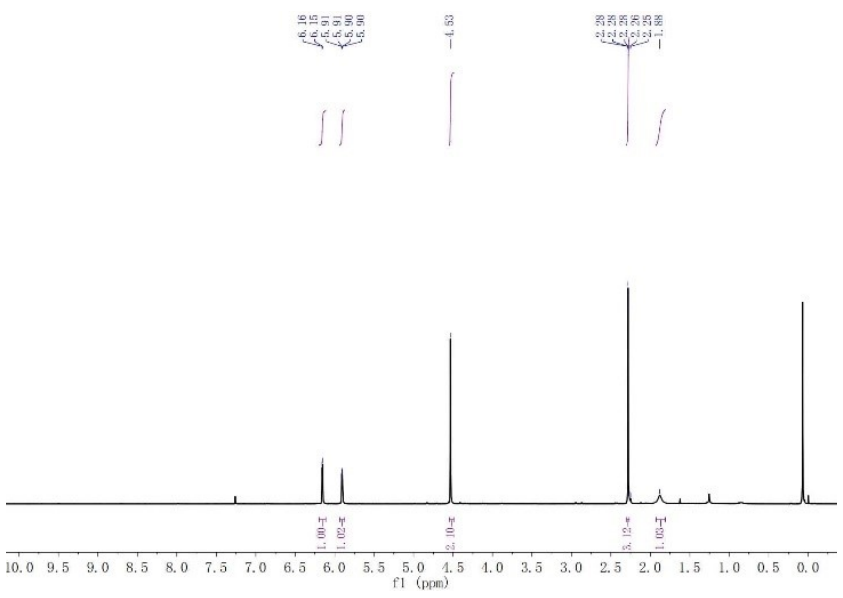
6.16
6.15
5.91
5.91
5.90
5.90
4.53
2.28
2.28
2.28
2.26
2.25
1.88
1.00
1.02
2.10
3.12
1.03
10.0 9.5 9.0 8.5 8.0 7.5 7.0 6.5 6.0 5.5 5.0 4.5 4.0 3.5 3.0 2.5 2.0 1.5 1.0 0.5 0.0
f1 (ppm)

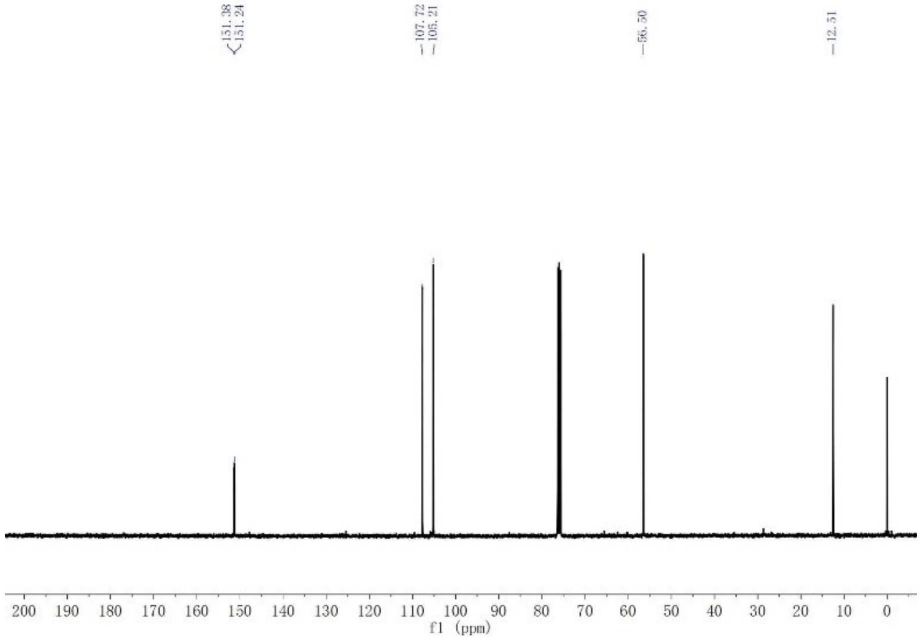
151.38
151.24
107.72
105.21
56.50
12.51
200 190 180 170 160 150 140 130 120 110 100 90 80 70 60 50 40 30 20 10 0
f1 (ppm)

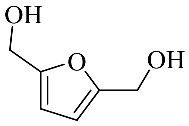
OH
O
OH

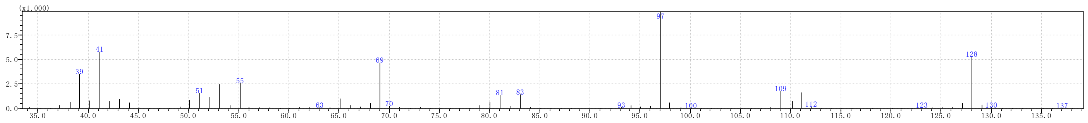
(x1,000)
7.5
5.0
2.5
0.0
39
41
51
55
63
69
70
81
83
93
97
100
109
112
123
128
130
137
35.0 40.0 45.0 50.0 55.0 60.0 65.0 70.0 75.0 80.0 85.0 90.0 95.0 100.0 105.0 110.0 115.0 120.0 125.0 130.0 135.0

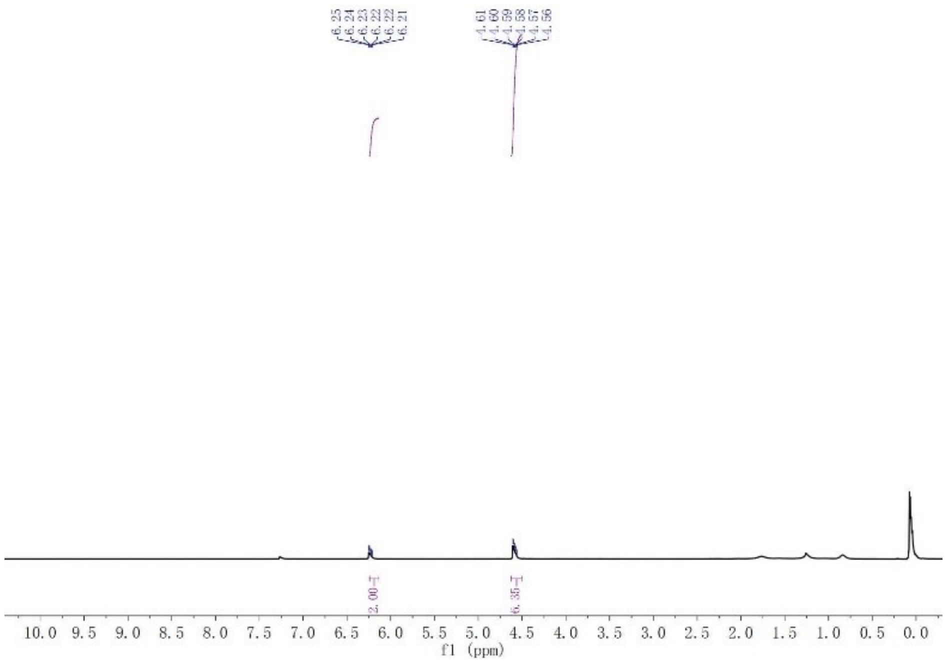
6.25
6.24
6.23
6.22
6.22
6.21
4.61
4.60
4.59
4.58
4.57
4.56
2.00
6.35
10.0 9.5 9.0 8.5 8.0 7.5 7.0 6.5 6.0 5.5 5.0 4.5 4.0 3.5 3.0 2.5 2.0 1.5 1.0 0.5 0.0
f1 (ppm)

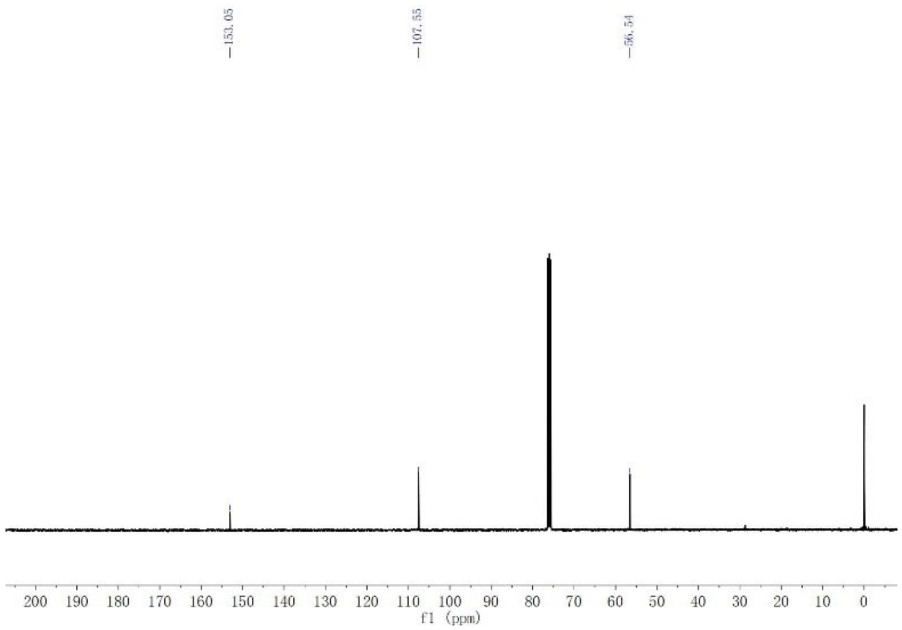
153.05
107.55
56.54
200 190 180 170 160 150 140 130 120 110 100 90 80 70 60 50 40 30 20 10 0
f1 (ppm)

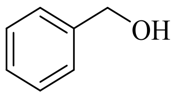
OH

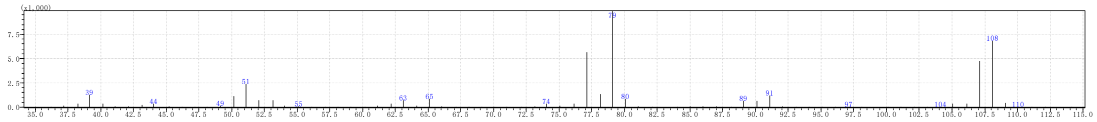
(x1,000)
7.5
5.0
2.5
0.0
39
44
49
51
55
63
65
74
79
80
89
91
97
104
108
110
35.0 37.5 40.0 42.5 45.0 47.5 50.0 52.5 55.0 57.5 60.0 62.5 65.0 67.5 70.0 72.5 75.0 77.5 80.0 82.5 85.0 87.5 90.0 92.5 95.0 97.5 100.0 102.5 105.0 107.5 110.0 112.5 115.0

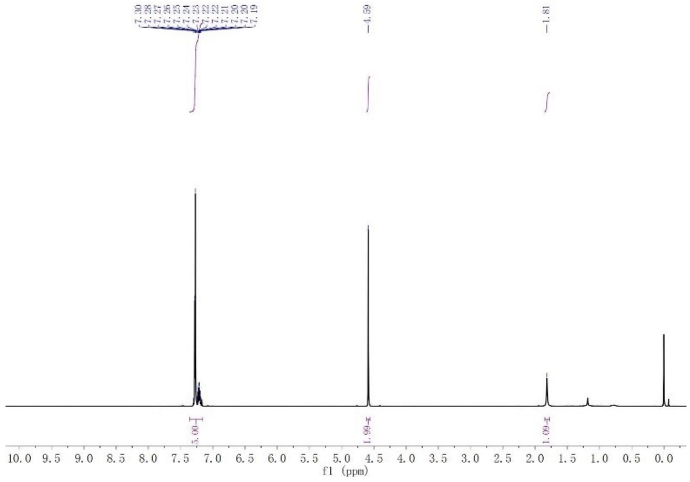
7.30
7.28
7.27
7.26
7.25
7.24
7.23
7.22
7.22
7.21
7.20
7.20
7.19
4.59
1.81
5.00
1.99
1.09
10.0 9.5 9.0 8.5 8.0 7.5 7.0 6.5 6.0 5.5 5.0 4.5 4.0 3.5 3.0 2.5 2.0 1.5 1.0 0.5 0.0
f1 (ppm)

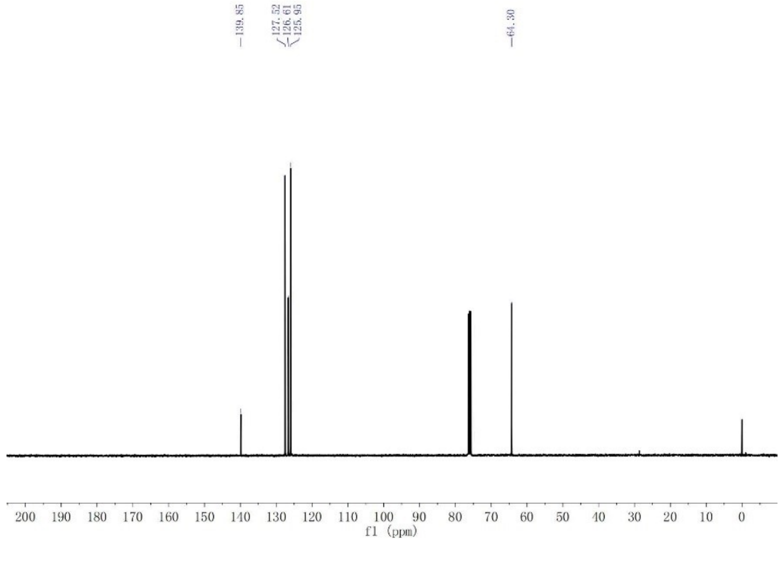
139.85
127.52
126.61
125.95
64.30
200 190 180 170 160 150 140 130 120 110 100 90 80 70 60 50 40 30 20 10 0
f1 (ppm)

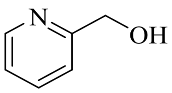
N
OH

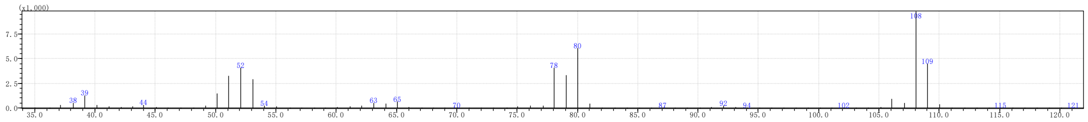
(x1,000)
7.5
5.0
2.5
0.0
38
39
44
52
54
63
65
70
78
80
87
92
94
102
108
109
115
121
35.0
40.0
45.0
50.0
55.0
60.0
65.0
70.0
75.0
80.0
85.0
90.0
95.0
100.0
105.0
110.0
115.0
120.0

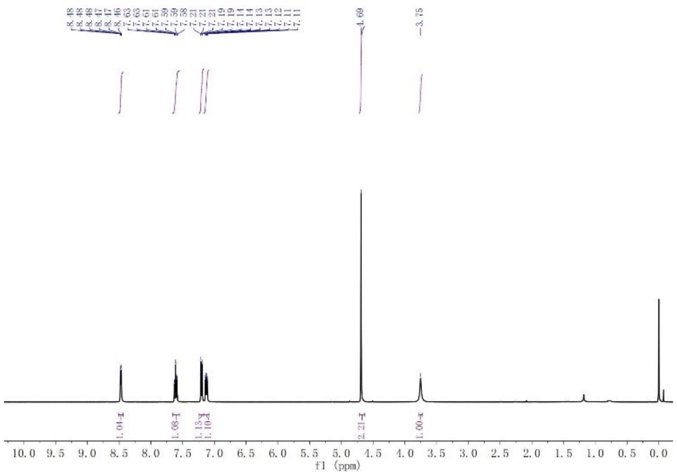
8.48
8.48
8.48
8.47
8.47
8.46
7.63
7.63
7.61
7.61
7.59
7.59
7.58
7.21
7.21
7.21
7.19
7.19
7.14
7.14
7.13
7.13
7.12
7.11
7.11
4.69
3.75
1.04
1.08
1.13
1.10
2.21
1.00
10.0
9.5
9.0
8.5
8.0
7.5
7.0
6.5
6.0
5.5
5.0
4.5
4.0
3.5
3.0
2.5
2.0
1.5
1.0
0.5
0.0
f1 (ppm)

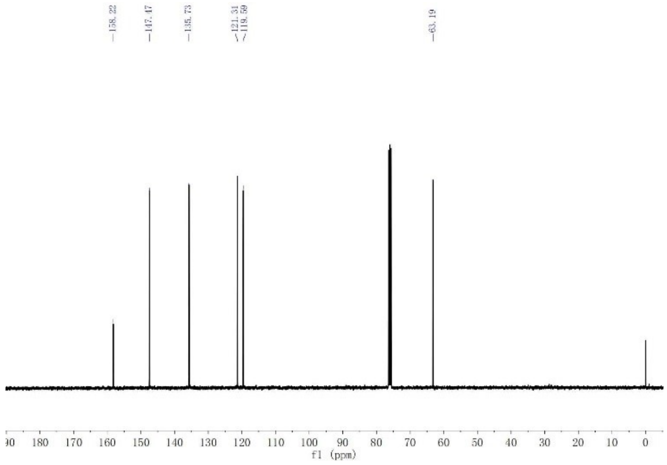
158.22
147.47
135.73
121.31
119.59
63.19
180
170
160
150
140
130
120
110
100
90
80
70
60
50
40
30
20
10
0
f1 (ppm)

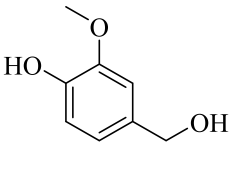
O
HO
OH

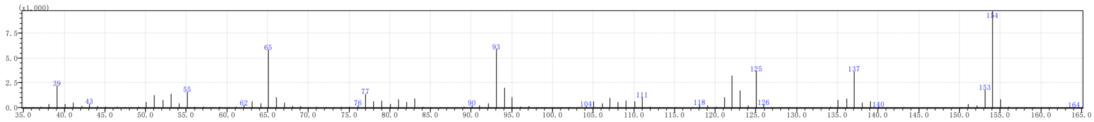
(x1,000)
7.5
5.0
2.5
0.0
39
43
55
62
65
76
77
90
93
104
111
118
125
126
137
140
153
154
164
35.0
40.0
45.0
50.0
55.0
60.0
65.0
70.0
75.0
80.0
85.0
90.0
95.0
100.0
105.0
110.0
115.0
120.0
125.0
130.0
135.0
140.0
145.0
150.0
155.0
160.0
165.0

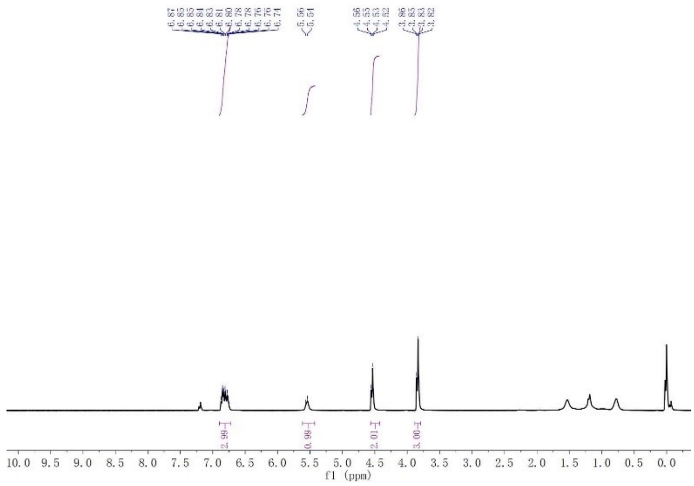
6.87 6.85 6.85 6.84 6.83 6.81 6.80 6.78 6.78 6.76 6.76 6.74
5.56 5.54
4.56 4.55 4.53 4.52
3.86 3.85 3.83 3.82
2.99
0.98
2.01
3.00
10.0 9.5 9.0 8.5 8.0 7.5 7.0 6.5 6.0 5.5 5.0 4.5 4.0 3.5 3.0 2.5 2.0 1.5 1.0 0.5 0.0
f1 (ppm)

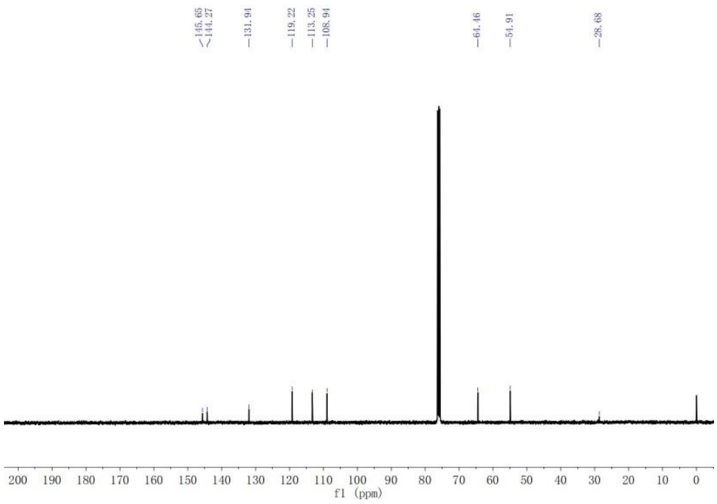
145.65
144.27
131.94
119.22
113.25
108.94
64.46
54.91
28.68
200 190 180 170 160 150 140 130 120 110 100 90 80 70 60 50 40 30 20 10 0
f1 (ppm)

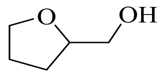
O
OH

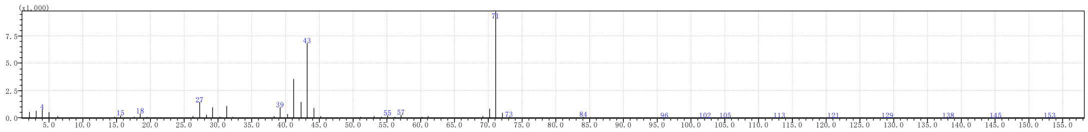
(x1,000)
7.5
5.0
2.5
0.0
4
15
18
27
39
43
55
57
71
73
84
96
102
105
113
121
129
138
145
153
5.0 10.0 15.0 20.0 25.0 30.0 35.0 40.0 45.0 50.0 55.0 60.0 65.0 70.0 75.0 80.0 85.0 90.0 95.0 100.0 105.0 110.0 115.0 120.0 125.0 130.0 135.0 140.0 145.0 150.0 155.0

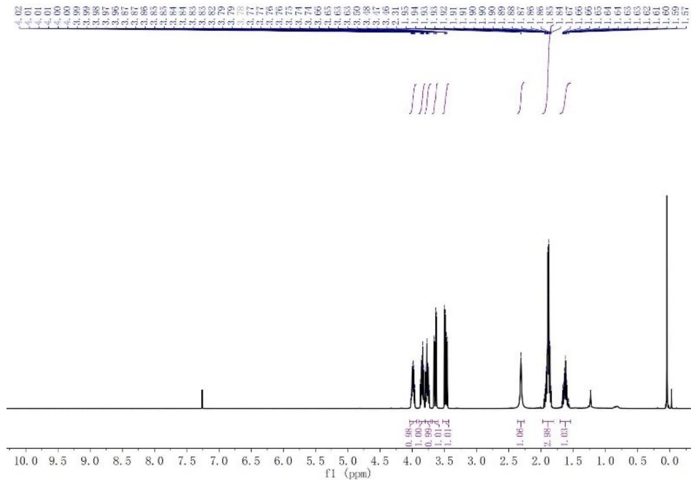
4.02 4.01 4.01 4.01 4.00 4.00 3.99 3.99 3.98 3.97 3.96 3.87 3.87 3.86 3.85 3.85 3.84 3.84 3.83 3.83 3.82 3.79 3.79 3.78 3.77 3.77 3.76 3.76 3.75 3.74 3.74 3.65 3.65 3.63 3.63 3.50 3.48 3.47 3.46 2.31 1.95 1.94 1.93 1.93 1.92 1.91 1.91 1.90 1.90 1.89 1.88 1.87 1.86 1.86 1.85 1.84 1.67 1.66 1.66 1.65 1.64 1.64 1.63 1.63 1.62 1.61 1.60 1.59 1.57
0.98
1.00
0.99
1.01
1.01
1.06
2.98
1.03
10.0 9.5 9.0 8.5 8.0 7.5 7.0 6.5 6.0 5.5 5.0 4.5 4.0 3.5 3.0 2.5 2.0 1.5 1.0 0.5 0.0
f1 (ppm)

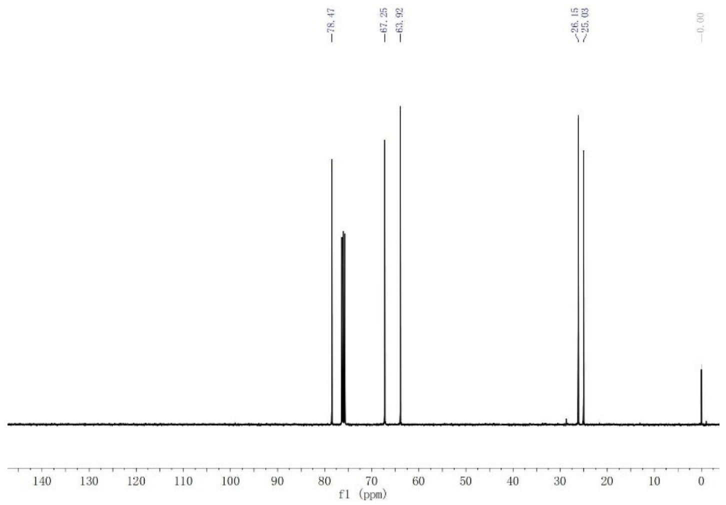
78.47
67.25
63.92
26.15
25.03
0.00
140 130 120 110 100 90 80 70 60 50 40 30 20 10 0
f1 (ppm)

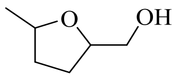
O
OH

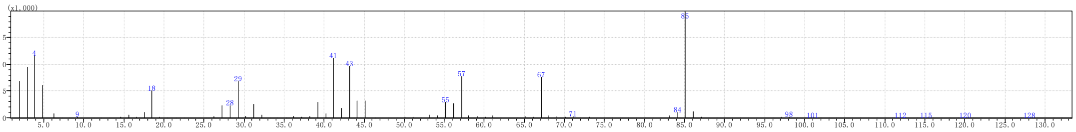
(x1,000)
7.5
5.0
2.5
0.0
4
9
18
28
29
41
43
55
57
67
71
84
85
98
101
112
115
120
128
5.0 10.0 15.0 20.0 25.0 30.0 35.0 40.0 45.0 50.0 55.0 60.0 65.0 70.0 75.0 80.0 85.0 90.0 95.0 100.0 105.0 110.0 115.0 120.0 125.0 130.0

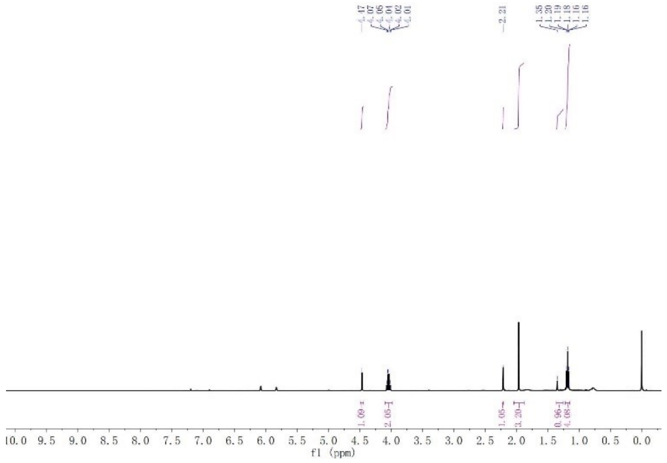
4.47
4.07
4.05
4.04
4.02
4.01
2.21
1.35
1.20
1.19
1.18
1.16
1.16
1.09
2.05
1.05
3.20
0.96
6.08
10.0 9.5 9.0 8.5 8.0 7.5 7.0 6.5 6.0 5.5 5.0 4.5 4.0 3.5 3.0 2.5 2.0 1.5 1.0 0.5 0.0
f1 (ppm)

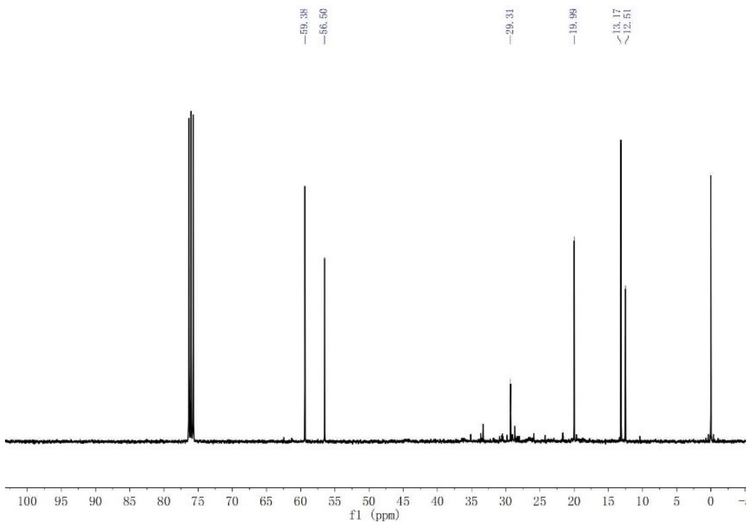
59.38
56.56
29.31
19.99
13.17
12.51
100 95 90 85 80 75 70 65 60 55 50 45 40 35 30 25 20 15 10 5 0
f1 (ppm)

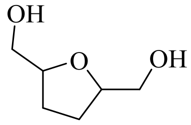
OH
O
OH

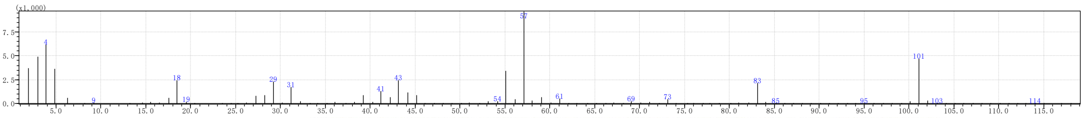
(x1,000)
7.5
5.0
2.5
0.0
5
9
18
19
29
31
41
43
54
57
61
69
73
83
85
95
101
103
114
5.0 10.0 15.0 20.0 25.0 30.0 35.0 40.0 45.0 50.0 55.0 60.0 65.0 70.0 75.0 80.0 85.0 90.0 95.0 100.0 105.0 110.0 115.0

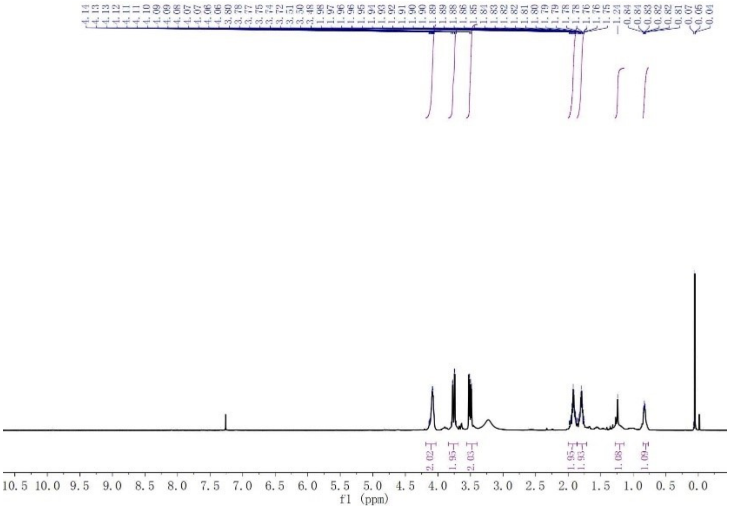
4.14 4.13 4.13 4.12 4.11 4.11 4.10 4.09 4.09 4.08 4.07 4.07 4.06 4.06 3.80 3.78 3.77 3.75 3.74 3.72 3.51 3.50 3.48 1.98 1.97 1.96 1.96 1.95 1.94 1.93 1.92 1.91 1.90 1.90 1.89 1.89 1.88 1.88 1.86 1.85 1.83 1.82 1.81 1.81 1.80 1.79 1.78 1.78 1.78 1.76 1.75 1.24 0.84 0.83 0.83 0.82 0.82 0.81 0.07 0.05 0.04
2.02
1.95
2.03
1.95
1.93
1.08
1.09
10.5 10.0 9.5 9.0 8.5 8.0 7.5 7.0 6.5 6.0 5.5 5.0 4.5 4.0 3.5 3.0 2.5 2.0 1.5 1.0 0.5 0.0
f1 (ppm)

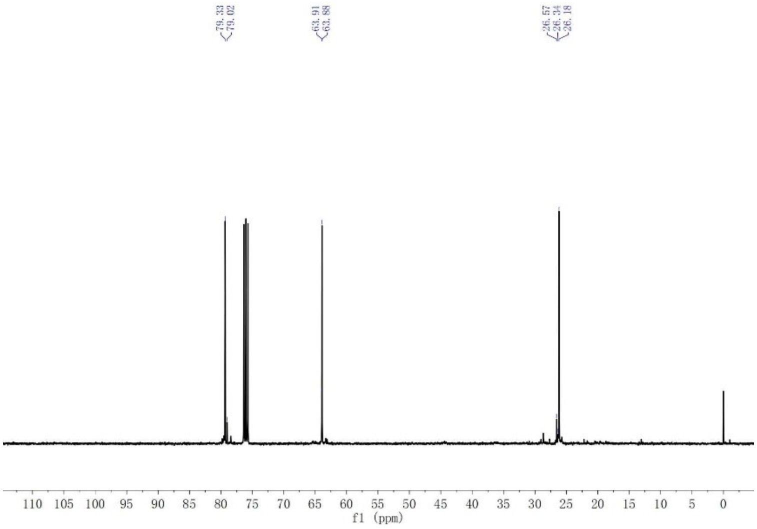
79.33
79.02
63.91
63.88
26.57
26.34
26.18
110 105 100 95 90 85 80 75 70 65 60 55 50 45 40 35 30 25 20 15 10 5 0
f1 (ppm)

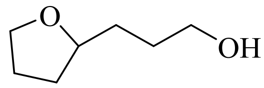
O
OH

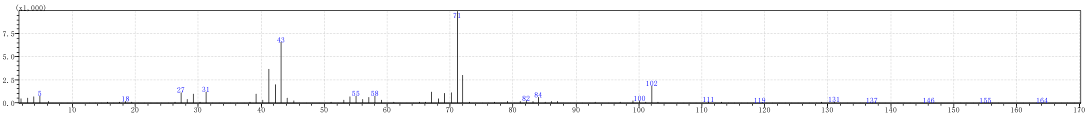
(x1,000)
7.5
5.0
2.5
0.0
5
18
27
31
43
55
58
71
82
84
100
102
111
119
131
137
146
155
164
10 20 30 40 50 60 70 80 90 100 110 120 130 140 150 160 170

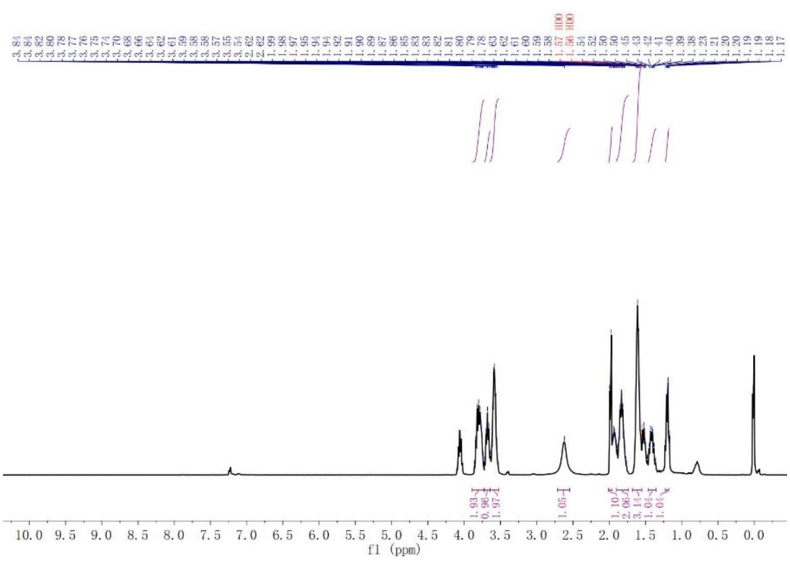
3.81 3.81 3.80 3.80 3.78 3.77 3.76 3.75 3.74 3.70 3.68 3.66 3.64 3.63 3.62 3.61 3.59 3.58 3.58 3.57 3.55 3.54 2.62 2.62 1.99 1.98 1.97 1.95 1.94 1.94 1.92 1.91 1.90 1.89 1.87 1.86 1.85 1.83 1.83 1.82 1.81 1.80 1.79 1.78 1.63 1.62 1.61 1.60 1.59 1.58 1.57 HDO 1.56 HDO 1.54 1.52 1.50 1.45 1.43 1.42 1.41 1.40 1.39 1.38 1.23 1.21 1.20 1.19 1.19 1.18 1.17
1.93
0.96
1.97
1.05
1.10
2.06
3.14
1.04
1.04
10.0 9.5 9.0 8.5 8.0 7.5 7.0 6.5 6.0 5.5 5.0 4.5 4.0 3.5 3.0 2.5 2.0 1.5 1.0 0.5 0.0
f1 (ppm)

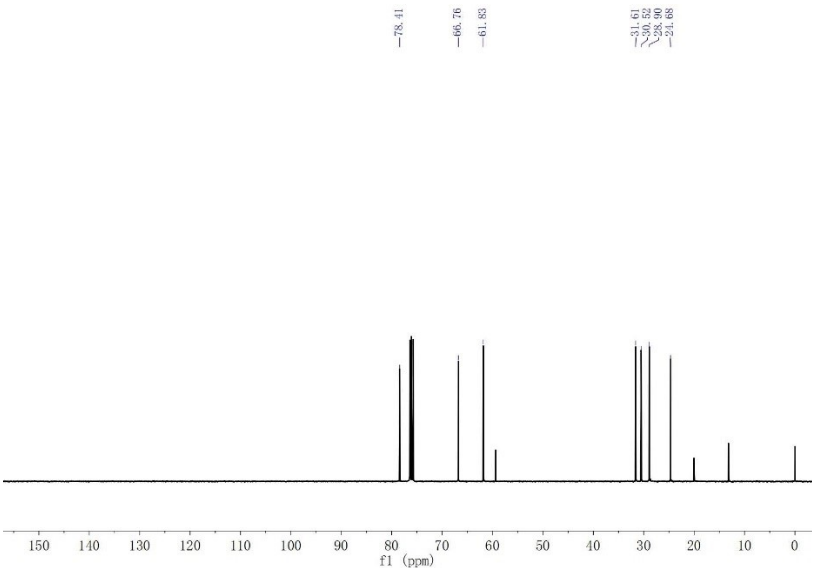
78.41
66.76
61.83
31.61
30.52
28.90
24.68
150
140
130
120
110
100
90
80
70
60
50
40
30
20
10
0
f1 (ppm)

9. References

1. Kresse, G.; Furthmuller, J. Efficient Iterative Schemes for Ab Initio Total-Energy Calculations Using a Plane-Wave Basis Set. *Phys. Rev. B* **1996**, *54*, 11169-11186.
2. Kresse, G.; Furthmuller, J. Efficiency of Ab-Initio Total Energy Calculation for Metals and Semiconductors Using a Plane-Wave Basis Set. *Comput. Mater. Sci.* **1996**, *6*, 15-50.
3. Grimme, S.; Antony, J.; Ehrlich, S.; Krieg, H. A Consistent and Accurate ab initio Parametrization of Density Functional Dispersion Correction (DFT-D) for the 94 Elements H-Pu. *J. Chem. Phys.*, **2010**, *132*, 154104.
4. Blöchl, P. E. Projector Augmented-Wave Method. *Phys. Rev. B* **1994**, *50*, 17953-17979.
5. Perdew, J. P.; Burke, K.; Ernzerhof, M. Generalized Gradient Approximation Made Simple. *Phys. Rev. Lett.* **1996**, *77*, 3865-3868.
6. Henkelman, G.; Jónsson, H. Improved Tangent Estimate in the Nudged Elastic Band Method for Finding Minimum Energy Paths and Saddle Points. *J. Chem. Phys.* **2000**, *113*, 9978-9985.
7. Henkelman, G.; Uberuaga, B. P.; Jónsson, H. A Climbing Image Nudged Elastic Band Method for Finding Saddle Points and Minimum Energy Paths. *J. Chem. Phys.* **2000**, *113*, 9901-9904.